Fig. 1. Amino acid sequence of rhFS. Predicted cleavage sites with Asp-N are indicated by |. The potential *N*-glycosylation sites are indicated by boxes.

pharmacokinetics, solubility, and protease resistance [13,14]. Glycosylation on FS is also likely to exert an effect on activin-neutralizing activity; however, neither structure of the N-linked oligosaccharides in FS, nor their physiological roles, have been clarified due to the limited availability of these oligosaccharides.

The aim of this study was to elucidate the glycosylation of FS. We previously developed an oligosaccharide profiling method using liquid chromatography/mass spectrometry (LC/MS) equipped with a graphitized carbon column (GCC) [15–22]. Recently, we demonstrated a procedure for facilitating the structural analysis of glycoproteins [16]. Carbohydrate profiles and site-specific glycosylations can be characterized by the GCC-LC/MS method, followed by mass spectrometric peptide/glycopeptide mapping. We used this method to demonstrate here the carbohydrate heterogeneity and the site-specific N-linked oligosaccharide structures in recombinant human FS288 (rhFS) produced in Chinese hamster ovary (CHO) cells, in which a sufficient amount of FS could be expressed.

2. Materials and methods

2.1. Materials

Human FS315 cDNA and recombinant human activin A were kindly provided by Dr. Yuzuru Eto (Ajinomoto Co., Inc., Kawasaki, Japan). CHO cells were obtained from the Japanese Cancer Research Resources Bank (Tokyo, Japan). Mammalian expression vector pcDNA3.1/Hygro was purchased from Invitrogen (Carlsbad, CA, USA). LipofectAMINE plus reagent, Ham's F12 medium, fetal calf serum (FCS) and hygromycin were purchased from Life Technologies Inc. (Rockville, MD, USA). Pellicon XL membrane and Immobilon-P membrane were purchased from Millipore Corp. (Bedford, MA, USA). Sulfated-cellulofine was purchased from Seikagaku Corp. (Tokyo, Japan). Neuraminidase was purchased from Nakalai Tesque (Kyoto, Japan). *N*-glycosidase F (PNGaseF) and endoproteinase Asp-N (Asp-N) were purchased from Boehringer Mannheim (Mannheim, Germany). All other chemicals were obtained from commercial sources and were of the highest purity available.

2.2. Establishment of a CHO cell line expressing rhFS

Complementary DNA encoding human FS288, was constructed from FS315 cDNA, and was cloned into pcDNA3.1/Hygro. This expression vector was transfected into CHO cells with LipofectAMINE plus reagent, according to the manufacturer's instructions. To screen the transformants, the transfectants were cultured with Ham's F12 medium supplemented with 10% FCS and 1 mg/ml hygromycin. After 2 weeks, the colonies were lifted with a micropipette. Expression levels of rhFS were assessed by an activin-neutralizing assay. The candidates were cloned by limiting dilution twice and were assessed again. The most productive rhFS-expressing clone (CHO-FS) was used in the following experiments.

2.3. Preparation of rhFS

Semi-confluent CHO-FS cells were cultured in Ham's F12 medium supplemented with 2% FCS. The conditioned medium was concentrated to a 1/10 volume by filtration with a Pellicon XL membrane (M_r 5000 cut), and was applied onto a sulfated-cellulofine column (2.5 × 20 cm) at 2 ml/min. The column was washed with 50 mM Tris–HCl (pH 8) containing 0.5 M NaCl, and the protein was eluted with 50 mM Tris–HCl (pH 8) containing 1.5 M NaCl. The effluent from the column was fractionated, and rhFS was monitored on Western blots using polyclonal anti-FS antibody. The fractions containing rhFS were injected into an HPLC (Hitachi D7000, Hitachi Co., Tokyo, Japan) apparatus equipped with a reversed-phase column (Vydac C4, 10 × 300 mm, The Separations Group, Inc., Hesperia, CA, USA). The protein was eluted with a linear gradient of 16–48% of acetonitrile/0.1% trifluoroacetic acid (TFA) for 30 min at a flow rate of 2 ml/min. Elution of proteins was monitored at 280 nm and individual peaks were manually collected. Fraction of rhFS was monitored on Western blots using polyclonal anti-FS antibody.

2.4. SDS-PAGE analysis of rhFS

RhFS was digested with or without PNGaseF at 37 °C for 24 h. The proteins were separated by sodium dodecyl sulfate-polyacrylamide gel electrophoresis

(SDS-PAGE) on 10% polyacrylamide gel. The gel was stained with Coomassie blue.

2.5. Isoelectric focusing

RhFS was dissolved in 100 mM ammonium acetate buffer, pH 4.5, and incubated with neuraminidase at 37 °C for 18 h. The proteins were precipitated with cold acetone and separated by isoelectric focusing (IEF). The gel was stained with Coomassie blue.

2.6. MALDI-TOF MS

RhFS (20 μg) was subjected to positive-ion matrix-assisted laser desorption/ionization time-of-flight mass spectrometry (MALDI-TOF MS), using a Shimazu/KRATOS MALDI I instrument (Shimazu Co., Kyoto, Japan) with 3,5-dimethoxy-4-hydroxy-cinnamic acid as the matrix.

2.7. Monosaccharide composition analysis

Monosaccharide composition analysis was performed according to the method reported by Hardy et al. [23]. Briefly, rhFS (50 μg) was hydrolyzed with 2 M TFA at 100 °C for 3 h. Monosaccharide compositions were analyzed by high-pH anion-exchange chromatography with pulsed amperometric detection (HPAEC-PAD) using a DX-300 system (Dionex, Sunnyvale, CA, USA) equipped with a CarboPac PA-1 anion exchange column (4 × 250 mm, Dionex).

2.8. Preparation of N-linked oligosaccharides alditols

N-linked oligosaccharides alditols were prepared by a previously described method [20]. Briefly, rhFS (100 μg) was digested with 5 units of PNGaseF at 37 °C for 2 days. Proteins were precipitated with 75% cold ethanol. The oligosaccharides were incubated with $NaBH_4$ at room temperature for 2 h. Excess reagent was decomposed with diluted acetic acid. The mixture was applied to a Supelclean ENVI-Carb column (Supelco, Bellefonte, PA, USA), which was washed with H_2O to remove the salts. Borohydride-reduced oligosaccharides were eluted with 30% acetonitrile/5 mM ammonium acetate.

2.9. Sugar profiling by LC/MS

Sugar profiling was carried out using a MAGIC 2002 system (Michrom BioResources, Inc., Auburn, CA, USA) connected to a TSQ7000 triple-stage quadruple mass spectrometer (ThermoFinnigan, San Jose, CA, USA) in the positive-ion mode. The column used was a GCC (Hypercarb 5 μm, 1.0 × 150 mm, ThermoFinnigan). The eluents were 5 mM ammonium acetate (pH 9.6) containing 2% acetonitrile (pump A); and 5 mM ammonium acetate (pH 9.6) containing 80% acetonitrile (pump B). The N-linked oligosaccharide alditols were eluted at a flow rate of 50 μl/min for 80 min with a gradient of 5–30% in pump B. The ESI voltage was set at 4500 V, and the capillary temperature was 175 °C. The electron multiplier was set at 1200 V.

2.10. Asp-N digestion

RhFS was reduced and *S*-carboxymethylated as previously described [20]. Briefly, rhFS (100 μg) was dissolved in 0.5 M Tris–HCl buffer (pH 8.6) containing 8 M guanidine and 5 mM EDTA. After reduction with 2-mercaptoethanol at room temperature for 2 h, monoiodoacetic acid was added and incubated at room temperature for 2 h in the dark. Reduced and *S*-carboxymethylated-rhFS (equivalent to 100 μg of rhFS) was digested with Asp-N (2 μg) in 25 mM NH_4HCO_3 (pH 8.0) at 37 °C for 20 h. The predicted peptides to be obtained by Asp-N digestion were sequentially designated as D1–D15 (Fig. 1).

2.11. Peptide/glycopeptide mapping of Asp-N-digested rhFS

Peptide/glycopeptide mapping was carried out using a MAGIC 2002 system connected to a TSQ7000 triple-stage quadruple mass spectrometer in the positive-ion mode. The column used was a MAGIC C18 column (1.0 × 150 mm, Michrom BioResources). The eluents were 2% acetonitrile/0.05% TFA (pump A), and 80% acetonitrile/0.05% TFA (pump B). Asp-N-digested rhFS was eluted with a linear gradient from 5 to 45% in pump B at a flow rate of 50 μl/min for 40 min. The eluate was monitored at 206 nm. The ESI voltage was set at 4500 V, and the capillary temperature was 175 °C. The electron multiplier was set at 1200 V. Precursor-ion scanning was performed using argon gas as the collision gas at a pressure of 2 mTorr. The collision energy was adjusted to −25 eV. The scan rate was 3 s/scan.

3. Results

3.1. Heterogeneity of rhFS

The carbohydrate heterogeneity of rhFS was analyzed by SDS-PAGE with and without PNGaseF digestion. The intact rhFS migrated as bands of an apparent molecular mass of 32 kDa and 33–36 kDa under non-reducing conditions (Fig. 2A, lane 1). PNGaseF digestion resulted in the disappearance of the multiple bands at 33–36 kDa with increases in the 32-kDa band (Fig. 2A, lane 2). These results suggest that the 32 kDa band and higher molecular weight bands are

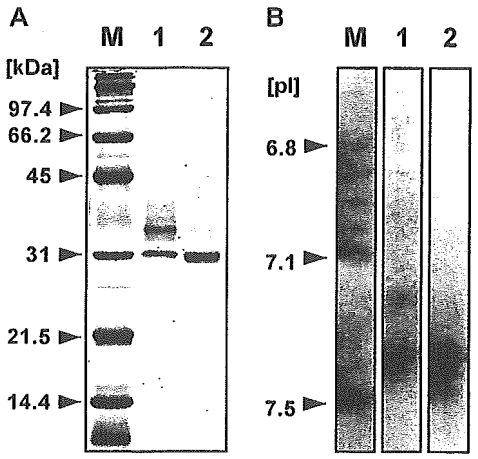

Fig. 2. (A) SDS-PAGE analysis of intact rhFS (lane 1) and PNGaseF-digested rhFS (lane 2). Lane M represents molecular weight markers. (B) IEF of intact rhFS (lane 1) and neuraminidase-digested rhFS (lane 2). Lane M represents p*I* markers.

the non-glycosylated FS and the glycosylated FS with diverse N-linked oligosaccharides, respectively.

The sialic acid heterogeneity of rhFS was analyzed by IEF with and without neuraminidase digestion. IEF of intact rhFS showed that the majority of the isoforms are located from p*I* 6.9 to 7.4 (Fig. 2B, lane 1). After treatment with neuraminidase, the acidic bands had disappeared and shifted at p*I* 7.4 (Fig. 2B, lane 2). These results suggested that the sialic acids contribute to the heterogeneity and the charge of rhFS.

The distribution of glycoforms was further investigated by MALDI-TOF MS. As shown in Fig. 3, multiple ions were detected in the range of 31.5–37 kDa. The most abundant ion at *m/z* 31,525 corresponded to the theoretical mass of non-glycosylated FS (31,514 Da). The other ions at *m/z* 33,804 and 35,600 could have been monoglycosylated FS and diglycosylated FS, respectively.

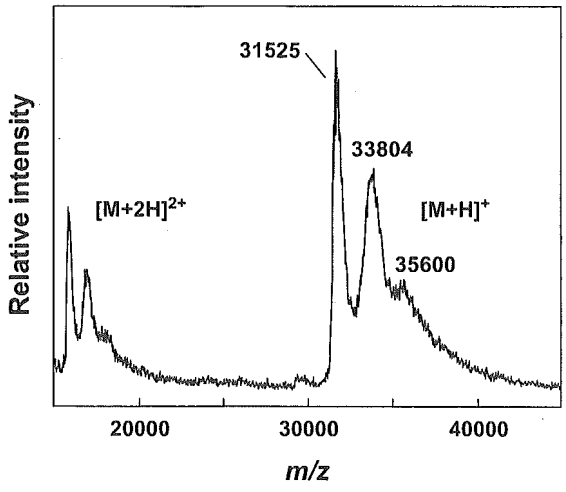

Fig. 3. MALDI-TOF MS analysis of intact rhFS. The peaks at *m/z* 31,525, 33,804 and 35,600 correspond to the non-glycosylated and glycosylated form of rhFS, respectively.

3.2. Monosaccharide composition of rhFS

Monosaccharide composition was analyzed by hydrolysis followed by HPAEC-PAD. The relative molecular ratio of fucose and glucosamine were estimated at 1.2 and 4.4, respectively, when mannose was considered as 3.0 (Table 1). This result suggests the presence of fucosylated bi- and triantennary-type oligosaccharides. No galactosamine residue was detected, suggesting the absence of O-linked oligosaccharides.

3.3. N-linked oligosaccharides in rhFS

N-linked oligosaccharides were released from rhFS by PNGaseF digestion and reduced with $NaBH_4$ to avoid the separation of anomers. Then the oligosaccharide alditols from rhFS were analyzed by GCC-LC/MS. Fig. 4 shows the total ion current chromatogram of N-linked oligosaccharide alditols. The *m/z* values of intense ions observed in major peaks (peaks 8 and 12) were 1040.7^{2+} and 1186.4^{2+}, which were consistent with the theoretical *m/z* values of $[dHex][Hex]_5[HexNAc]_4[NeuAc]^{2+}$ and $[dHex][Hex]_5[HexNAc]_4[NeuAc]_2{}^{2+}$, respectively (Table 2). The elution times of these oligosaccharides were in good agreement with those of fucosyl biantennary oligosaccharides bearing mono- and di-NeuAc prepared from erythropoietin, respectively [24]. An ion at *m/z* 1041.4^{2+} was also detected in peak 6. This oligosaccharide could be a sialylation isomer of peak 8 (1040.7^{2+}).

Likewise, the ions at *m/z* 1790.7^{+} and 895.4^{2+} in peak 2 and at *m/z* 1077.9^{2+} in peak 3 were assigned as an asialo fucosylated biantennary oligosaccharide and an asialo fucosylated triantennary oligosaccharide, respectively. The ion at *m/z* 2389.6^{+} and 1194.6^{2+} in peak 11 was consistent with $[dHex][Hex]_5[HexNAc]_4[NeuAc][NeuGc]^{2+}$ or $[Hex]_6[HexNAc]_4[NeuAc]_2{}^{2+}$, respectively. The ions at *m/z* 2097.7^{+} and 1048.6^{2+} in peak 5 and at *m/z* 2096.5^{+} and 1049.5^{2+} in peak 8 were consistent with $[dHex][Hex]_5[HexNAc]_4[NeuGc]^{2+}$ or $[Hex]_6[HexNAc]_4[NeuAc]^{2+}$, respectively. The minor ions at *m/z* 1224.1^{2+}, 1224.3^{2+}, 1369.7^{2+}, 1369.8^{2+},

Table 1
Monosaccharide composition analysis of rhFS oligosaccharides

Monosaccharide	Relative molar proportions[a]
Fucose	1.2
Galactosamine	0.3
Glucosamine	4.4
Galactose	3.2
Glucose	0.3
Mannose	3.0

[a] Data are normalized to three-mannose residues.

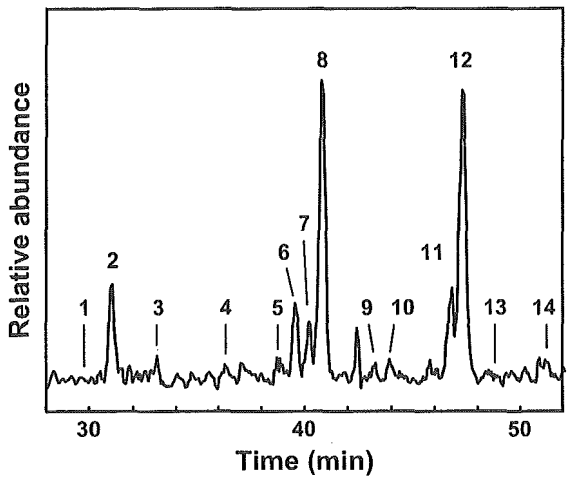

Fig. 4. Sugar map of oligosaccharide alditols released from rhFS. N-linked oligosaccharide alditols from rhFS were separated with GCC. The total ion content was scanned using the positive-ion mode at *m/z* 700–2400.

1370.5^{2+} and 1515.5^{2+} in peaks 7, 9, 11, 12, 13 and 14 were deduced to the fucosylated triantennary oligosaccharides with NeuAc, respectively.

The ratio of oligosaccharides was estimated as follows: fucosylated biantennary, ca. 85%, and fucosylated triantennary structures, ca. 10%, based on their ion currents; these results were in good agreement with the results of the monosaccharide composition analysis.

3.4. Site-specific glycosylation of rhFS

FS contains two potential *N*-glycosylation sites (Asn95 and Asn259, Fig. 1). The site-specific glycosylation and other post-translational modifications, such as phosphorylation and hydroxylation, were analyzed by mass spectrometric peptide/glycopeptide mapping (Fig. 5a, Table 3). Most of the non-glycosylated peptides were detected except for the small peptides, i.e. peptides D2 (tripeptide), D13 (tetrapeptide), and D12 (pentapeptide), which suggests the absence of *O*-glycans and any post-translational modifications on these peptides. The small peptides have no putative *N*-glycosylation site (Fig. 1), and no galactosamine residue was detected (Table 1). These findings suggest the absence of N- and O-linked oligosaccharides. However, the possibility remains that the small peptides are modified, such as by phosphorylation. Two unpredicted peptides (*m/z* 1176.2^{2+} and 510.4^{2+}) were detected among the Asp-N digests of rhFS. They were assigned to peptides D15-1 and D15-2, which were produced from peptide D15 by further cleavage at the amino-terminal of Glu280. It was reported that a cleavage at the N-terminal site of glutamic acid is a possible cut site for Asp-N under the same conditions [25]. Peptides D5 and D15-1, each of which have potential glycosylation site, were detected as non-glycosylated forms in the peptide/glycopeptide map.

Table 2
Putative structures of N-linked oligosaccharides deduced from the GCC-LC/MS

Peak No.[a]	Carbohydrate structure[b]	Theoretical mass[c]	Observed mass[d]		
			M^+	M^{2+}	M^{3+}
1		1627.5	1628.3	814.2	-
2		1789.7	1790.7	895.4	-
3		2155.0	-	1077.9	-
4		1934.7	-	967.9	-
5	*1	2096.9	2097.7	1048.6	-
6		2080.9	2081.2	1041.4	-
7		2446.3	-	1224.1	817.4
8	*1	2096.9	2096.5	1049.6	-
		2080.9	2082.2	1040.7	-
9		2446.3	-	1224.3	-
10		2226.0	-	1114.2	-
11	*2	2388.2	2389.6	1194.6	-
		2737.5	-	1369.7	913.4
12		2372.2	2372.2	1186.4	-
		2737.5	-	1369.8	-
13		2737.5	-	1370.5	913.8
14		3028.8	-	1515.5	-

Note: The observed *m/z* of *1 and *2 are also consistent with the theoretical *m/z* value of $[Hex]_6[HexNAc]_4[NeuAc]$ and $[Hex]_6[HexNAc]_4[NeuAc]_2$, respectively.

[a] Peak label in Fig. 4.

[b] Proposed structures based on molecular weight. Symbols: solid squares, GlcNAc; open circles, mannose; open diamonds, galactose; dotted diamonds, fucose; solid circle, NeuAc; dotted circle, NeuGc.

[c] Calculated average mass.

[d] Mass of the ion measured in the positive-ion ESI mass spectrum from alditols.

Precursor-ion scanning, which can detect $[Hex][HexNAc]^+$ at *m/z* 366 produced by collision-induced dissociation, was performed for the monitoring of the glycopeptides. The TIC chromatogram of the precursor-ion scanning showed two significant peaks, peaks G1 and G2 (Fig. 5b). Fig. 6 shows the mass spectra of peaks G1 and G2 in Fig. 5b. On the basis of the theoretical masses of the peptides and oligosaccharides identified by sugar mapping (Table 2), peaks G1 and G2

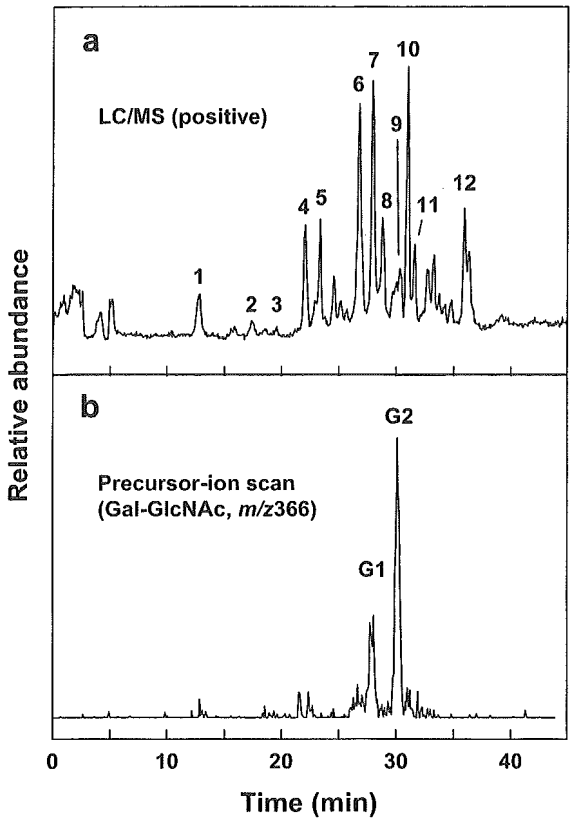

Fig. 5. Peptide/glycopeptide map of the rhFS Asp-N digest. The total ion current chromatogram of LC/MS in the positive-ion mode at m/z 400–2400 (a), and the TIC chromatogram of LC/MS/MS, precursor-ion scan of m/z 366 (b).

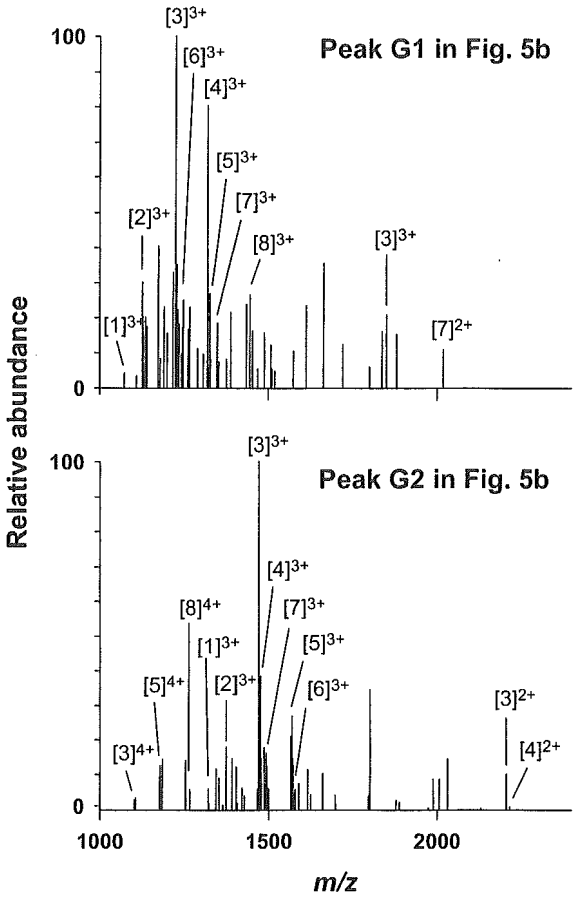

Fig. 6. Mass spectra of glycopeptides in peaks G1 and G2 in Fig. 5b. The observed m/z value of each ion is summarized in Table 4.

were assigned to glycosylated D5 and D15-1, respectively. The oligosaccharides attached to each *N*-glycosylation site were deduced as shown in Table 4. By comparing the N-linked oligosaccharide structures on Asn95 with those on Asn259, it was concluded that biantennary oligosaccharides are major oligosaccharides located at both Asn95 and Asn259, whereas the triantennary structures are present mainly at Asn95.

Table 3
Assignment of the peaks in Fig. 5a

Peak no.[a]	Peptide[b]	Theoretical mass[c]	Observed m/z[d]					
			M^{+}	M^{2+}	M^{3+}	M^{4+}	M^{5+}	M^{6+}
1	D4	2666.0	–	1334.2	889.9	667.4	–	–
2	D14	777.8	778.6	–	–	–	–	–
3	D15-2[e]	1018.0	1019.0	510.4	–	–	–	–
4	D11	1456.6	1457.5	729.0	486.3	–	–	–
5	D6	4378.8	–	–	1460.8	1095.5	–	–
6	D8	3326.4	–	1664.6	1109.5	–	–	–
	D10	1467.6	1468.2	734.8	490.1	–	–	–
7	D1	4728.1	–	–	1577.0	1183.2	947.0	789.6
8	D7	1329.4	1330.2	665.3	–	–	–	–
9	D5	1608.7	1609.3	805.1	–	–	–	–
10	D9	4165.6	–	–	1389.0	1042.2	834.1	–
11	D15-1[e]	2350.6	–	1176.2	784.2	–	–	–
12	D3	3219.5	–	1610.1	1073.8	806.4	–	–

[a] Peak label in Fig. 5a.
[b] Predicted peptides were shown in Fig. 1.
[c] Calculated average mass.
[d] Mass of the ions measured in the positive-ion ESI mass spectrum from precursor-ion scan.
[e] Peptide derived from D15 peptide.

4. Discussion

The aim of the present study was to analyze the distribution of the glycoforms and the carbohydrate structures of rhFS. Previous study of FS isolated from porcine ovary has shown that porcine FS exists in six isoforms, due to alternative splicing and the site occupancy of N-linked oligosaccharides [8]. In this study, we used rhFS288 to eliminate the heterogeneity due to alternative splicing. The results of SDS-PAGE and MALDI-TOF MS revealed the presence of both non-glycosylated and glycosylated forms (Figs. 2 and 3). FS contains two potential *N*-glycosylation sites. Using mass spectrometric peptide/glycopeptide mapping and precursor-ion scanning, we found that both *N*-glycosylation sites were partially glycosylated (Fig. 5 and Table 3). Non-glycosylated and glycosylated proteins containing Asn95 and Asn259 were detected in the peptide/glycopeptide map and precursor-ion scanning, respectively. Monosaccharide composition analyses suggested the presence of linkages of fucosylated bi- and triantennary complex-type oligosaccharides on rhFS (Table 1). This finding was supported by mass spectrometric oligosaccharide profiling, in which the *m/z* values and elution times of some of the oligosaccharides from rhFS were in good agreement with those of standard oligosaccharides. The site-specific glycosylations were deduced on the basis of the mass spectra of glycopeptides. It was suggested that biantennary oligosaccharides attach to both Asn95 and Asn259, whereas triantennary oligosaccharides attach mainly to Asn95 (Fig. 6 and Table 4).

Asn95 is located in the follistatin domain I, which is thought to be the heparin-binding site [26]. The site occupancy and structure of N-linked oligosaccharides on Asn95 may affect the heparin-binding ability of FS. Heparin/heparan sulfate proteoglycans are known to exert an important influence on FS, which neutralizes the activity of activins. It is therefore possible that sialylated oligosaccharides at Asn95 control the activin-neutralizing activity via modulation of the heparin-binding ability of FS. In fact, it was reported that the *N*-glycosylation isoforms of antithrombin and heparin cofactor II differ substantially in their affinity for heparin [27,28]. We are currently studying the role played by oligosaccharides in the activin-neutralizing activity of FS; these studies employ the carbohydrate remodeling technique using the CHO cell line established in the present study.

Table 4
Putative structures of N-linked oligosaccharides deduced from the LC/MS of the glycopeptides corresponding to the Asn95 and Asn259

Carbohydrate Structure[a]	Asn95					Asn259				
	Ions in peak G1	Theoretical mass[b]	Observed *m/z*[c]			Ions in peak G2	Theoretical mass[b]	Observed *m/z*		
			M^{2+}	M^{3+}	M^{4+}			M^{2+}	M^{3+}	M^{4+}
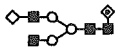	1	3216.2	-	1073.4	-	1	3958.1	-	1319.6	-
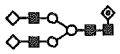	2	3378.6	-	1126.6	-	2	4120.5	-	1373.9	-
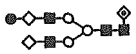	3	3669.6	1835.7	1223.2	-	3	4411.5	2206.3	1471.8	1104.7
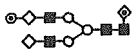	-		-		-	4	4427.5	2214.8	1475.7	-
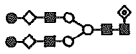	4	3960.9	-	1320.6	-	5	4702.8	-	1569.5	1177.1
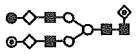	5	3976.6	-	1326.8	-	6	4718.8	-	1574.5	-
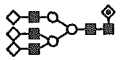	6	3743.7	-	1248.6	-	7	4485.6	-	1497.2	-
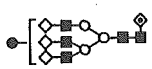	7	4034.9	2017.5	1346.9	-	-	-	-	-	-
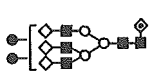	8	4326.2	-	1444.1	-	8	5068.1	-	-	1267.6

[a] Proposed structures based on molecular weight. Symbols: solid squares, GlcNAc; open circles, mannose; open diamonds, galactose; dotted diamonds, fucose; solid circle, NeuAc; dotted circle, NeuGc.

[b] Calculated average mass.

[c] Mass of the ion measured in the positive-ion ESI mass spectrum from precursor-ion scan. Mass spectra were shown in Fig. 6.

Acknowledgements

We thank Dr. Y. Eto (Ajinomoto Co., Inc.) for providing the human FS315 cDNA. This work was supported by a grant-in-aid for the Research on Health Sciences Focusing on Drug Innovation from the Japan Health Sciences Foundation.

References

[1] Robertson DM, Klein R, de Vos FL, McLachlan RI, Wettenhall RE, Hearn MT, et al. The isolation of polypeptides with FSH suppressing activity from bovine follicular fluid which are structurally different to inhibin. Biochem Biophys Res Commun 1987;149:744–9.

[2] Ueno N, Ling N, Ying SY, Esch F, Shimasaki S, Guillemin R. Isolation and partial characterization of follistatin: a single-chain Mr 35,000 monomeric protein that inhibits the release of follicle-stimulating hormone. Proc Natl Acad Sci USA 1987;84: 8282–6.

[3] Nakamura T, Takio K, Eto Y, Shibai H, Titani K, Sugino H. Activin-binding protein from rat ovary is follistatin. Science 1990; 247:836–8.

[4] Kogawa K, Nakamura T, Sugino K, Takio K, Titani K, Sugino H. Activin-binding protein is present in pituitary. Endocrinology 1991;128:1434–40.

[5] Massague J. The transforming growth factor-beta family. Annu Rev Cell Biol 1990;6:597–641.

[6] Kingsley DM. The TGF-beta superfamily: new members, new receptors, and new genetic tests of function in different organisms. Genes Dev 1994;8:133–46.

[7] Wada M, Shintani Y, Kosaka M, Sano T, Hizawa K, Saito S. Immunohistochemical localization of activin A and follistatin in human tissues. Endocr J 1996;43:375–85.

[8] Sugino K, Kurosawa N, Nakamura T, Takio K, Shimasaki S, Ling N, et al. Molecular heterogeneity of follistatin, an activin-binding protein. Higher affinity of the carboxyl-terminal truncated forms for heparan sulfate proteoglycans on the ovarian granulosa cell. J Biol Chem 1993;268:15579–87.

[9] Patel K. Follistatin. Int J Biochem Cell Biol 1998;30:1087–93.

[10] Inouye S, Guo Y, DePaolo L, Shimonaka M, Ling N, Shimasaki S. Recombinant expression of human follistatin with 315 and 288 amino acids: chemical and biological comparison with native porcine follistatin. Endocrinology 1991;129:815–22.

[11] Sumitomo S, Inouye S, Liu XJ, Ling N, Shimasaki S. The heparin binding site of follistatin is involved in its interaction with activin. Biochem Biophys Res Commun 1995;208:1–9.

[12] Hashimoto O, Nakamura T, Shoji H, Shimasaki S, Hayashi Y, Sugino H. A novel role of follistatin, an activin-binding protein, in the inhibition of activin action in rat pituitary cells. Endocytotic degradation of activin and its acceleration by follistatin associated with cell-surface heparan sulfate. J Biol Chem 1997;272: 13835–42.

[13] Kobata A. Structures and functions of the sugar chains of glycoproteins. Eur J Biochem 1992;209:483–501.

[14] Varki A. Biological roles of oligosaccharides: all of the theories are correct. Glycobiology 1993;3:97–130.

[15] Itoh S, Kawasaki N, Ohta M, Hyuga M, Hyuga S, Hayakawa T. Study on evaluating methods for the quality control of glycoprotein products. (III)—Erythropoietin products. Part 3. Bull Natl Inst Health Sci 2001;65–9.

[16] Simultaneous microanalysis of N-linked oligosaccharides in a glycoprotein using microbore graphitized carbon column liquid chromatography–mass spectrometry. J Chromatogr A 2002;968: 89–100.

[17] Kawasaki N, Ohta M, Hyuga S, Hashimoto O, Hayakawa T. Analysis of carbohydrate heterogeneity in a glycoprotein using liquid chromatography/mass spectrometry and liquid chromatography with tandem mass spectrometry. Anal Biochem 1999;269: 297–303.

[18] Kawasaki N, Ohta M, Hyuga S, Hyuga M, Hayakawa T. Application of liquid chromatography/mass spectrometry and liquid chromatography with tandem mass spectrometry to the analysis of the site-specific carbohydrate heterogeneity in erythropoietin. Anal Biochem 2000;285:82–91.

[19] Kawasaki N, Haishima Y, Ohta M, Itoh S, Hyuga M, Hyuga S, et al. Structural analysis of sulfated N-linked oligosaccharides in erythropoietin. Glycobiology 2001;11:1043–9.

[20] Kawasaki N, Ohta M, Itoh S, Hyuga M, Hyuga S, Hayakawa T. Usefulness of sugar mapping by liquid chromatography/mass spectrometry in comparability assessments of glycoprotein products. Biologicals 2002;30:113–23.

[21] Ohta M, Kawasaki N, Hyuga S, Hyuga M, Hayakawa T. Selective glycopeptide mapping of erythropoietin by on-line high-performance liquid chromatography–electrospray ionization mass spectrometry. J Chromatogr A 2001;910:1–11.

[22] Ohta M, Kawasaki N, Itoh S, Hayakawa T. Usefulness of glycopeptide mapping by liquid chromatography/mass spectrometry in comparability assessment of glycoprotein products. Biologicals 2002;30:235–44.

[23] Hardy MR, Townsend RR, Lee YC. Monosaccharide analysis of glycoconjugates by anion exchange chromatography with pulsed amperometric detection. Anal Biochem 1988;170:54–62.

[24] Kawasaki N, Ohta M, Hyuga S, Hyuga M, Hayakawa T. Application of liquid chromatography/mass spectrometry and liquid chromatography with tandem mass spectrometry to the analysis of the site-specific carbohydrate heterogeneity in erythropoietin. Anal Biochem 2000;285:82–91.

[25] Ingrosso D, Fowler AV, Bleibaum J, Clarke S. Specificity of endoproteinase Asp-N (Pseudomonas fragi): cleavage at glutamyl residues in two proteins. Biochem Biophys Res Commun 1989; 162:1528–34.

[26] Inouye S, Ling N, Shimasaki S. Localization of the heparin binding site of follistatin. Mol Cell Endocrinol 1992;90:1–6.

[27] Picard V, Ersdal-Badju E, Bock SC. Partial glycosylation of antithrombin III asparagine-135 is caused by the serine in the third position of its *N*-glycosylation consensus sequence and is responsible for production of the beta-antithrombin III isoform with enhanced heparin affinity. Biochemistry 1995;34:8433–40.

[28] Bohme C, Nimtz M, Grabenhorst E, Conradt HS, Strathmann A, Ragg H. Tyrosine sulfation and *N*-glycosylation of human heparin cofactor II from plasma and recombinant Chinese hamster ovary cells and their effects on heparin binding. Eur J Biochem 2002;269:977–88.

J. Biochem. **137**, 579–586 (2005)
DOI: 10.1093/jb/mvi070

Thrombomodulin Enhances the Invasive Activity of Mouse Mammary Tumor Cells

Shingo Niimi[1,*], Mizuho Harashima[2], Kazuko Takayama[2], Mayumi Hara[2], Masashi Hyuga[1], Taiichiro Seki[2], Toyohiko Ariga[2], Toru Kawanishi[1] and Takao Hayakawa[3]

[1]Division of Biological Chemistry and Biologicals, National Institute of Health Sciences, Kamiyoga 1-18-1, Setagaya-ku, Tokyo 158-8501; [2]Department of Nutrition and Physiology, Nihon University College of Bioresource Sciences, Kameino, Fujisawa 252-8510; and [3]Deputy Director General, National Institute of Health Sciences, Kamiyoga 1-18-1, Setagaya-ku, Tokyo 158-8501

Received January 31, 2005; accepted February 18, 2005

Thrombomodulin (TM) is a thrombin receptor on the surface of endothelial cells that converts thrombin from a procoagulant to an anticoagulant. Thrombin promotes invasion by various tumor cells, and positive or negative correlations are found between the expression of TM and tumorigenesis in some patients. In this study, we used an invasion assay to investigate the effect of TM on the invasive activity of a mouse mammary tumor cell line, MMT cells, and the effects of TM were compared with those of thrombin as a positive control. In the presence of 1% fetal calf serum (FCS), TM significantly stimulated MMT cell invasion in a dose-dependent manner, resulting in an approximately 3-fold increase at 1–10 pg/ml over the untreated control. Thrombin also caused a similar degree of stimulation at 50 ng/ml. Since thrombin activity was detected in the components of the assay system, an invasion assay was also performed in a thrombin-activity-depleted assay system constructed to eliminate the effect of thrombin activity; TM (10 pg/ml) plus thrombin (1 pg/ml) stimulated invasion by approximately 3.5-fold in this assay system. Hirudin, a specific thrombin inhibitor, inhibited stimulation by TM as well as by thrombin in both the presence and absence of 1% FCS. Investigations of the effects of TM on proliferation, adhesion and chemotaxis to clarify the mechanism of stimulation by TM revealed that TM does not affect proliferation or adhesion in the presence of 1% FCS, but stimulates chemotaxis by approximately 2.3-fold. Similar results were obtained in experiments using thrombin. TM (10 pg/ml) plus thrombin (1 pg/ml), on the other hand, stimulated chemotaxis by approximately 2.3-fold in the thrombin-activity-depleted assay system. Binding studies using [^{125}I]-thrombin revealed that the cells have specific saturable binding sites for thrombin. These results show that TM stimulates the invasive activity of MMT cells, probably by acting as a cofactor for the thrombin-stimulated invasion of the cells *via* its receptor and lowering the effective concentration of thrombin. The findings also indicate that the stimulation of invasive activity in the presence of 1% FCS and in the thrombin-activity-depleted assay system may mainly be mediated by the stimulation of chemotaxis.

Key words: invasion, thrombin, thrombomodulin.

Abbreviations: TM, thrombomodulin; MEM, modified Eagle's medium; CS, calf serum; FCS, fetal calf serum; MMP, matrix metalloprotease; ECM, extracellular matrix; Boc-Asp(Obzl)-pro-Arg-MCA, Boc-β-benzyl-Asp-Pro-Arg-4-methyl-coumaryl-7-amide; PBS, phosphate-buffered saline.

Thrombomodulin (TM) is a thrombin receptor on the surface of endothelial cells (*1*) that was first discovered as a cofactor for the thrombin-catalyzed activation of the anticoagulant protein C (*2*). Biologically active soluble forms of TM, which probably represent the products of limited proteolytic cleavage of cell-surface TM, were later detected in human plasma (*3*), suggesting a possible role of the soluble forms *in vivo*. TM also positively or negatively regulates various functions of thrombin as described below. TM stimulates the inactivation of pro-urokinase-type plasminogen activator (*4*), the activation of TAF I (*5*), and the activation of progelatinase A (*6*). TM inhibits the activation of platelets (*7*), the activation of factor X (*8*) and human endothelial cells (*9*), the stimulation of fibrin formation (*8*), and the proliferation of arterial smooth muscle cells (*10*) and human umbilical vein endothelial cells (*11*).

On the other hand, there are several direct and indirect lines of evidence indicating that thrombin stimulates invasion and/or metastasis by tumor cells (*12–18*), and it has recently been reported that the expression of TM is increased or decreased in some carcinomas. The expression of TM increases in squamous carcinomas of the lung (*19*), colorectal carcinomas (*20*), and some transitional

*To whom correspondence should be addressed. Tel: +81-3-3700-9347, Fax: +81-3-3700-9084, E-mail: niimi@nihs.go.jp

carcinomas (*21–22*), and its expression level is negatively correlated with the malignancy of carcinoma of the esophagus (*23*), hepatocellular carcinoma (*24*), and ovarian tumors (*25*). There is also evidence of increased serum levels of TM in some tumors, including pancreatic cancer (*26*), digestive tract carcinoma (*27*), and glioblastoma (*28*). Based on this evidence, it is likely that TM plays some role in the regulation of tumor metastasis.

In this study, we investigated the effects of TM on the invasive activity of a mouse mammary tumor cell line, MMT, by an *in vitro* invasion assay, because tumor cell invasion through the basement membrane is a critical step in the process of metastasis (*29–30*). We also compared the effects of TM with those of thrombin as a positive control.

MATERIALS AND METHODS

Materials—TM was a kind gift of Asahi Kasei Pharma, Japan. The TM was prepared as described by Gomi *et al.* (*31*). Plasmids containing the cDNA encoding TM (residues 1–498) were transfected into COS-1 cells, and the recombinant TM was purified from serum-free COS-1-cell-conditioned medium. The purified TM yielded a single band at 90 kDa in SDS-PAGE under reducing conditions. The recombinant TM was confirmed to be thrombin-free by a protein C activating assay developed in our laboratory (*32*). Thrombin (1,140 units/mg protein) was a kind gift of Mochida Pharmaceutical Co., Ltd., Japan. Hirudin was purchased from Wako (Osaka, Japan). A fluorogenic substrate, Boc-β-benzyl-Asp-Pro-Arg-4-methyl-coumaryl-7-amide (Boc-Asp(Obzl)-pro-Arg-MCA), was purchased from Peptide Institute, Inc. (Osaka, Japan).

Cell Culture—MMT mouse mammary tumor cells were obtained from the Japanese Health Science Research Resource Bank and cultured in modified Eagle's medium (MEM) supplemented with 10% calf serum (CS) on 60-mm diameter culture dishes, 4×10^5 cells per dish. After 7 d, the subconfluent MMT cells were detached from the culture dishes with 0.25% trypsin/EDTA, treated with MEM containing 10% CS, and collected by centrifugation. The cells were then washed with MEM and used in experiments. In some experiments, the thrombin activity associated with cells was depleted as described below, and the resultant cells were used for various experiments in which MEM containing 0.1% BSA was used as the basal medium. We refer to this assay system as the thrombin-activity-depleted assay system below. To deplete thrombin activity, the cell suspension (1.5×10^5 cells in 10 ml of MEM) was incubated in a non-adherent form on 100-mm diameter non-treated culture dishes pre-coated with BSA (10 mg/ml) for 2 h in a humidified chamber at 37°C under 5% CO_2, and then washed with MEM.

In Vitro Invasion Assay—In vitro invasion by MMT cells was measured in a Matrigel invasion chamber (Collaborative Biomedical Products, Bedford, MA, USA). The chamber (upper compartment) was placed in a 24-well culture plate (lower compartment), and the cell suspension (1.6×10^5 cells in 500 μl) and the basal medium (750 μl) containing various factors were added to the upper and lower compartments, respectively. MEM containing 1% fetal calf serum (FCS) or 0.1% BSA was used as the basal medium. Matrigel invasion chambers were precoated with fibronectin as described below before use in the thrombin-activity-depleted assay system. Human plasma fibronectin solution (IWAKI, Japan) was diluted to a final concentration of 5 μg/ml with phosphate-buffered saline (PBS), and a 300 μl aliquot was added to the chamber and a 750 μl aliquot to the 24-well culture plate. The chamber and 24-well plate were allowed to stand at 37°C for 2 h and were then washed with PBS. After incubating the cells for 18 h, the filters were fixed with methanol and stained with hematoxylin and eosin. The cells on the upper surface of the filters were removed by wiping with cotton swabs, and the number of cells that had migrated to the lower surface of the filters was counted under a microscope.

Measurement of Thrombin Activity—Thrombin activity in FCS, CS, and on cells was measured by the method of Kawabata *et al.* (*33*). A 10 μl volume of 10% FCS or CS was mixed with 90 μl of reaction buffer containing 50 mM Tris-HCl, pH 8.0, 100 mM NaCl, and 10 mM $CaCl_2$, with or without hirudin (0.5 unit/ml). Packed cells (1×10^6 cells) were suspended in 100 μl of reaction buffer with or without hirudin (0.5 unit/ml). After adding 1 μl of 10 mM substrate, Boc-Asp(Obzl)-pro-Arg-MCA solution to the cell suspension, the mixture was incubated for 20 min at 37°C, and the reaction was stopped by adding 600 μl of 0.6 M acetic acid. The fluorescence of the aminomethylcoumarine released was measured with a fluorospectrophotometer at an excitation wavelength of 380 nm and an emission of 460 nm. A blank solution was prepared by adding 1 μl of substrate solution to the reaction buffer mixed with 600 μl of 0.6 M acetic acid. Thrombin activity was calculated using 1, 2.5, 5 and 10 ng/ml thrombin solutions as standards and subtracting the fluorescence obtained in the presence of hirudin from that in the absence of hirudin. A linear dose-response curve was obtained between 0.5–5 ng/ml of thrombin, and its activity was inhibited by more than 98% by hirudin (0.5 unit/ml). The fluorescence of each sample was within the linear range.

Proliferation Assay—The cell suspension (1×10^5 cells in 4 ml) was seeded on 60-mm diameter culture dishes and incubated with each factor for 18 h. MEM containing 1% FCS was used as the basal medium. The cells were then detached from the culture dishes with 0.25% trypsin/EDTA, treated with MEM containing 10% CS, collected by centrifugation, and counted with a hemocytometer.

Adhesion Assay—Adhesion assays were performed by a modification of the method of Deryugina *et al.* (*34*). A 300 μl aliquot of fibronectin (5 μg/ml), prepared as described above, was added to each well of 24-well plates (IWAKI, Japan). The plates were allowed to stand overnight at 4°C, washed with PBS, blocked with 1% BSA in PBS for 1 h at 37°C, and finally washed in PBS. MMT cells (55×10^4 cells) were exposed to each factor in 2 ml of MEM containing 1% FCS for 30 min at 37°C. After washing with 2 ml of MEM, the cell suspensions (1×10^5 cells in 0.38 ml of MEM) were seeded on each well. After incubation for 30 min at 37°C, non-adherent cells were removed by washing with PBS, and the adherent cells were fixed and stained with 0.2% crystal violet in 10% ethanol for 10 min. After three washes with 2 ml of PBS,

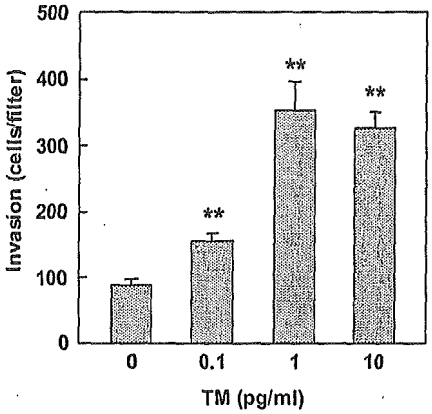

Fig. 1. **Dose dependency of the effect of TM on invasiveness.** MEM containing 1% FCS was used as the basal medium. The concentrations of TM indicated are the concentrations in the lower compartment. The data shown are means ± SD of the data obtained in duplicate wells in three experiments (**$p < 0.01$ *vs.* control). The deviation in each experiment was less than 10%.

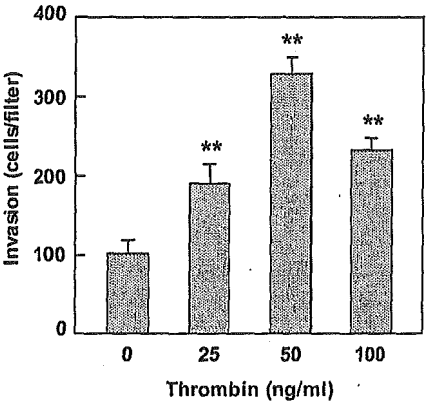

Fig. 2. **Dose dependency of the effect of thrombin on invasiveness.** MEM containing 1% FCS was used as the basal medium. The concentrations of thrombin indicated are the concentrations in the lower compartment. The data shown are means ± SD of data obtained in duplicate wells in three experiments (**$p < 0.01$ *vs.* control). The deviation in each experiment was less than 10%.

the dye was extracted in an end-over-end mixer with 600 μl of 50% ethanol in 50 mM sodium phosphate (pH 4.5) for 10 min, and absorbance was measured at 540 nm. The correlation between absorbance and cell number was confirmed in a preliminary experiment.

Chemotaxis Assay—Chemotaxis assays were performed with control inserts (Collaborative Biomedical Products, Bedford, MA, USA) in a similar manner to the invasion assay described above. The control inserts were not coated with Matrigel. MEM containing 1% FCS was used as the basal medium. The control inserts were pre-coated with fibronectin (5 μg/ml) as described for the pre-coating of the Matrigel invasion chamber in the thrombin-activity-depleted assay system.

Iodination of Thrombin and Determination of Binding—Thrombin was iodinated to a specific activity of 19.1 × 10^7 cpm/μg by the chloramine T method as described previously (*35–36*). After precoating 24-well plates with fibronectin (5 μg/ml) as described above, the cell suspensions (1.22 × 10^5 cells in 0.45 ml of MEM) were seeded into each well and incubated in a humidified chamber at 37°C under 5% CO_2 for 2 h. The cells were then washed with 0.4 ml of MEM containing 15 mM Hepes (pH 7.2) and 0.1% BSA and incubated for 1.5 h at 37°C in the same buffer with various concentrations of [^{125}I]-thrombin in the presence or absence of a 100-fold excess amount of unlabeled thrombin. After washing the cells four times with the same ice-cold buffer, the cells were solubilized with 0.4 ml of 1 N NaOH for 1 h at 37°C. Specific binding was calculated as the difference between total binding and nonspecific binding.

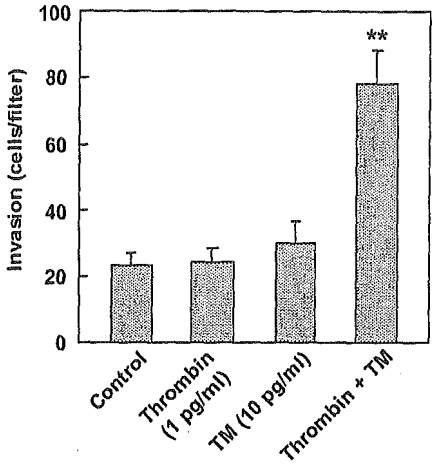

Fig. 3. **Effect of TM and thrombin on invasiveness in the thrombin-activity-depleted assay system.** Cells on which thrombin activity was depleted were used in the experiment. MEM containing 0.1% BSA was used as the basal medium. The data shown are means ± SD of data obtained in duplicate wells in three experiments (**$p < 0.01$ *vs.* control). The deviation in each experiment was less than 10%.

RESULTS

Effect of TM on Invasiveness—Figure 1 shows the effects of TM on the invasive activity of MMT cells in the presence of 1% FCS. TM significantly stimulated invasive activity in a dose-dependent manner, resulting in an approximately 3-fold stimulation at 1–10 pg/ml. Figure 2 shows the effects of thrombin used as a positive control. Thrombin also stimulated invasive activity in a dose-dependent manner.

On the basis of these findings, we investigated the possibility that the stimulation of invasion by TM might be dependent on thrombin that may have been introduced into the assay system as described below. First, thrombin activity in the assay system was measured. The thrombin concentrations in freshly prepared 10% FCS and CS measured by the thrombin activity assay were 200 pg/ml and 2.8 ng/ml, respectively. The amount of thrombin on the cells measured in a similar manner was 35 pg/10^6 cells. Based on these values, the thrombin concentrations in the assay system with or without 1% FCS were estimated to be 24.48 and 4.48 pg/ml, respectively. Second, the action of TM was examined in the thrombin-activity-depleted assay system described in "MATERIALS AND METHODS," and depletion of thrombin activity in the

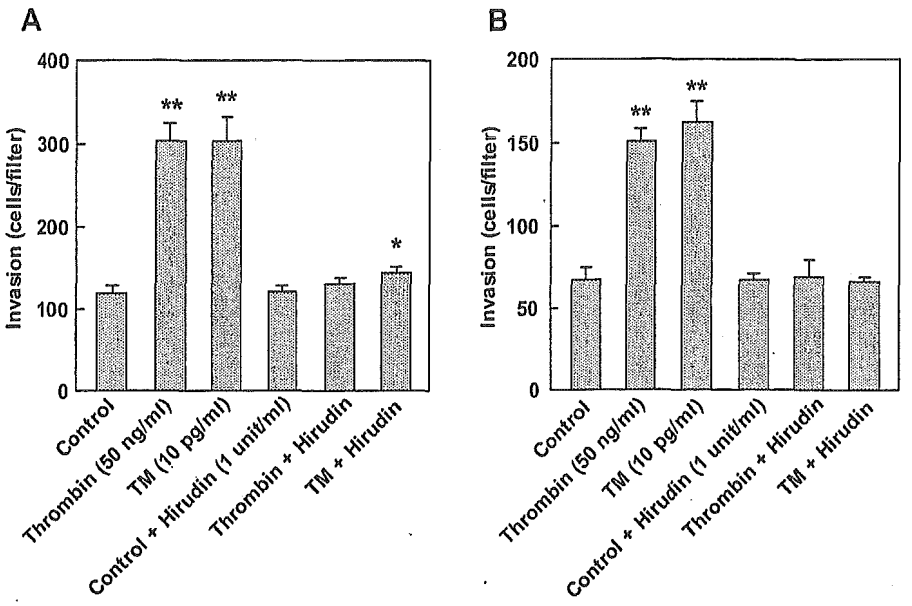

Fig. 4. **Effect of hirudin on the stimulation of invasion by TM.** (A) MEM containing 1% FCS was used as the basal medium. The indicated concentration of each factor is that in the lower compartment. The data shown are means ± SD of data obtained in duplicate wells in three experiments (*$p < 0.05$ *vs.* control; **$p < 0.01$ *vs.* control) (B) MEM containing 0.1% BSA was used as the basal medium. The data shown are means ± SD of data obtained in duplicate wells in three experiments (**$p < 0.01$ *vs.* control). The deviation in each experiment was less than 10%.

assay system was confirmed by the absence of any detectable thrombin activity on the cells. Figure 3 shows the effects of thrombin (1 pg/ml) and TM (10 pg/ml) on the invasive activity of cells in the thrombin-activity-depleted assay system. While neither thrombin or TM had any effect on invasion, TM plus thrombin stimulated invasion by approximately 3-fold.

Effect of Hirudin on the Stimulation of Invasion by TM—The action of TM was also examined in the presence of the specific thrombin inhibitor hirudin to investigate the possibility described above. Fig. 4, A and B, shows the effects of hirudin on the invasion-stimulating activity of TM in the presence and absence of 1% FCS. We used a 1 unit/ml concentration of hirudin in this experiment, because 50 ng/ml thrombin corresponds to 0.057 unit/ml, and so 1 unit/ml hirudin seemed adequate to inhibit this concentration of thrombin. As expected, hirudin (1 unit/ml) not only inhibited the stimulation by thrombin to control levels, but the stimulation by TM as well.

Effect of TM on Proliferation—Since tumor cell invasion consists of a series of events, including adhesion to the extracellular matrix (ECM) and chemotaxis, we investigated the effects of TM on these two events to clarify the molecular mechanism of the stimulation of invasive activity by TM. Before investigating the effect of TM on these processes, we investigated its effects on cell proliferation to confirm that the stimulation of invasive activity by TM is not an artifact of the enhancement of cell proliferation.

Figure 5 shows the effects of TM on MMT cell proliferation in the presence of 1% FCS. The numbers of cells in the presence of TM or thrombin did not differ from the numbers in the control cultures.

Effect of TM on Adhesion to Fibronectin—Figure 6 shows the effects of TM on adhesion to fibronectin, a basal lam-

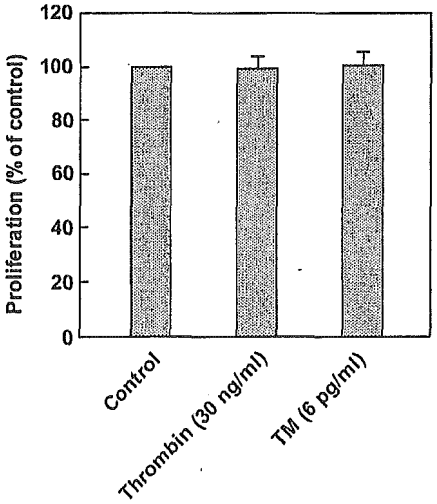

Fig. 5. **Effect of TM on proliferation.** MEM containing 1% FCS was used as the basal medium. The data shown are means ± SD of data obtained in duplicate dishes in three experiments. The deviation in each experiment was less than 10%.

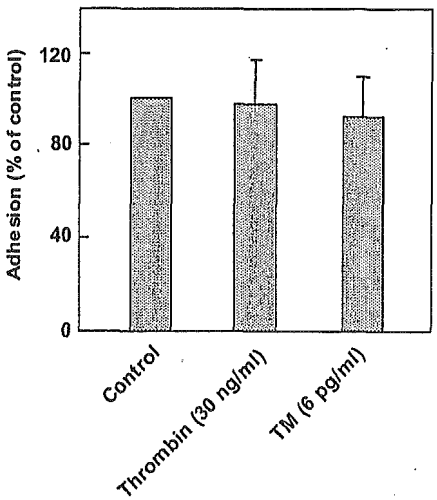

Fig. 6. **Effect of TM on adhesion to fibronectin.** MEM containing 1% FCS was used as the basal medium. The data shown are means ± SD of data obtained in duplicate wells in three experiments. The deviation in each experiment was less than 10%.

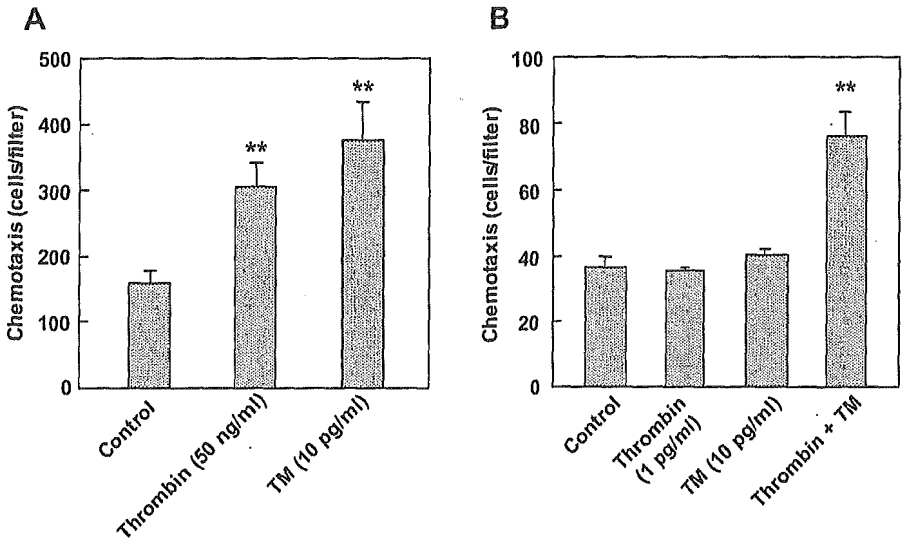

Fig. 7. **Effect of TM on chemotaxis.** (A) MEM containing 1% FCS was used as the basal medium. The data shown are means ± SD of data obtained in duplicate wells in three experiments (**$p < 0.01$ *vs.* control). (B) Cells on which thrombin activity was depleted were used in the experiment. MEM containing 0.1% BSA was used as the basal medium. The data shown are means ± SD of data obtained in duplicate wells in three experiments (**$p < 0.01$ *vs.* control). The deviation in each experiment was less than 10%.

ina component. Neither TM nor thrombin affected adhesion to fibronectin.

Effect of TM on Chemotaxis—Figure 7 (A and B), shows the effects of TM on chemotaxis by MMT cells in the presence of 1% FCS and in the thrombin-activity-depleted assay system, respectively. Both TM (10 pg/ml) and thrombin (50 ng/ml) significantly stimulated chemotaxis by MMT cells by approximately 1.9–2.3-fold in the former system, but neither TM (10 pg/ml) nor thrombin (1 pg/ml) affected chemotaxis in the latter system; TM plus thrombin, on the other hand, stimulated chemotaxis by approximately 2-fold.

Binding of Thrombin—Figure 8 shows the binding curves for specific [^{125}I]-thrombin binding sites on cells in the presence and absence of TM (10 pg/ml). These binding curves show the specific [^{125}I]-thrombin binding to be saturable at approximately 40 ng/ml, and that TM has no effect on the specific binding of [^{125}I]-thrombin. A similar binding experiment was performed in the [^{125}I]-thrombin concentration range of 1–10 pg/ml, but no specific binding was detected independent of the presence or absence of TM, probably because the absolute amount of radioactivity used was too low to be detected as specific binding.

DISCUSSION

In the present study, we show that, at its maximum effective dose, TM stimulates the invasive activity of MMT cells *in vitro* by approximately 3-fold. As far as we know, this is the first time that TM has been shown to stimulate the invasive activity of tumor cells *in vitro*. Similarly, exogenous thrombin causes maximal stimulation of invasion at 50 ng/ml, which is a concentration more than 1,000-fold higher than the maximum effective dose of TM.

Since TM acts as a cofactor for the thrombin-catalyzed activation of protein C and increases the rate of the reaction by >1,000-fold (*8*), the stimulation by TM may have been due to TM interacting with thrombin, which had been introduced into the assay system, and acting as a cofactor for thrombin-stimulated invasion of MMT cells, thus lowering the effective concentration of thrombin. This possibility seems to be supported by the detection of thrombin activity in the assay systems, the requirement for thrombin for stimulation by TM in the thrombin-activity-depleted assay system, and the inhibition of stimulation by hirudin. It is noteworthy that the thrombin concentration required for stimulation by TM in the thrombin-activity-depleted assay system is more than 20,000-fold less than the concentration required for thrombin to stimulate invasion. On the other hand, the control level was not inhibited by hirudin in the presence of 1% FCS, probably due to the lower thrombin concentration in the assay system compared with the effective concentration of exogenous thrombin.

There have been two studies examining the effect of TM on the invasive activity of tumor cells. Matsushita *et al.* showed that a subcloned human esophageal squamous cell carcinoma line with low TM expression is more invasive than a high TM-expressing clone (*37*). In their study, the action of TM does not seem to be due to an acceleration of its thrombin cofactor activity, because the difference between the cell lines with low and high TM expression with respect to their cofactor activity for protein C activation by thrombin was less than 13% and significantly lower than their TM levels and invasive activities. Hosaka *et al.* showed that TM (10–100 ng/ml)

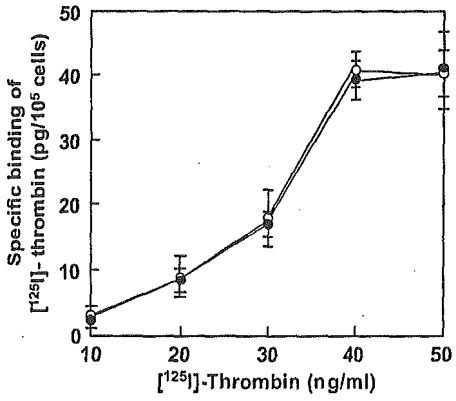

Fig. 8. **Binding of [^{125}I]-thrombin.** Specific binding of [^{125}I]-thrombin to cells in the absence (solid circles) and presence of TM (10 pg/ml) (open circles) was measured. The data shown are representative specific binding curves for [^{125}I]-thrombin binding sites and are means ± SD of data obtained in triplicate wells.

inhibits the invasive activity of mouse melanoma cells *in vitro* (*38*), and TM has also been found to decrease the proliferation of tumor cell lines subcloned from patients with malignant melanomas (*39*). None of these inhibitory effects were inhibited by hirudin.

In contrast to these studies, the present study shows that TM enhances the invasive activity of MMT cells and indicates that the action of TM is entirely dependent on thrombin as described above. Therefore, the mode and mechanism of action of TM in MMT cells seems to be different from its mode and mechanism of action in the squamous cell carcinoma line and melanoma cells.

It is useful to speculate on the role of TM in tumorigenesis based on the findings of our study, because tumor cell invasion through the basement membrane is a critical step in the process of metastasis (*29–30*). Several studies have shown that TM levels in serum increase in patients with certain tumors (*26–28*), as described in the Introduction. Thus, the results of this study suggest that the soluble form of TM may play a positive role in the malignancy of some kinds of tumors, probably by enhancing the metastatic potential of thrombin. On the other hand, TM on the cell surface may act as a negative regulator to thrombin, because thrombin is degraded as the thrombin-TM complex by its internalization after binding to TM on the cell surface (*40*). This possibility may be supported by the findings that the expression level of TM is negatively correlated with the malignancy of some carcinomas (*23–25*), as described in the Introduction.

Tumor cell invasion is a complex process that involves adhesion to ECM, degradation of ECM, and chemotaxis (*41*). Chemotaxis is the essential step in invasion as reviewed by Wells (*42*). The results of the present study show that both TM and thrombin stimulate chemotaxis in the presence of 1% FCS, and that TM plus thrombin stimulate chemotaxis in the thrombin-activity-depleted assay system. Both of these findings are consistent with previous reports that thrombin stimulates chemotaxis (*17*, *18*), and the presence of specific binding sites for thrombin on cells indicates that these actions are mediated by thrombin receptors.

However, other actions of thrombin may also be involved in the stimulation of tumor cell invasion, because the enhancement of chemotaxis alone is insufficient to account for the increase in tumor cell invasion. One such other possible action of thrombin is the stimulation of the matrix metalloprotease (MMP)–mediated degradation of a variety of ECM proteins, including collagens type IV, V, VII, and X, fibronectin, laminin (*43–47*), elastin (*48–49*), proteoglycans (*49–51*), and entactin (*52*). Several reports have indicated that thrombin increases the active forms of MMP-2 and MMP-9 (*53–59*), and plays important roles in the enhancement of tumor cell invasion and metastasis (*34*, *60–68*). There are also reports that thrombin stimulates the release of MMP-2 (*69*), the expression of MMP-1 and MMP-3 (*70*), and the expression of MMP-9 mRNA (*71*). Another possible action is the stimulation of MMP-independent degradation of ECM. This possibility appears to be supported by the finding that thrombin stimulates the expression of urokinase-type plasminogen activator, a factor involved in the degradation of ECM protein (*72*), and stimulates the heparinase-mediated release of heparan sulfate from ECM (*73*).

In conclusion, the results of this study show that TM stimulates the invasive activity of MMT cells, probably by acting as a cofactor for the thrombin-stimulated invasion of cells mediated by thrombin receptors, and by lowering the effective concentration of thrombin. Further, the results indicate that the stimulation is mainly caused by an enhancement of chemotaxis.

This study was supported, in part, by a Grant-in-Aid for research on health sciences focusing on drug innovation from the Japan Health Sciences Foundation.

REFERENCES

1. Esmon, C.T. and Owen, W.G. (1981) Identification of an endothelial cell cofactor for thrombin-catalyzed activation of protein C. *Proc. Natl Acad. Sci. USA* **78**, 2249–2252
2. Esmon, C.T. (1989) The roles of protein C and thrombomodulin in the regulation of blood coagulation. *J. Biol. Chem.* **264**, 4743–4746
3. Ishii, H. and Majerus, P.W. (1985) Thrombomodulin is present in human plasma and urine. *J. Clin. Invest.* **76**, 2178–2181
4. Molinari, A., Giorgetti, C., Lansen, J., Vaghi, F., Orsini, G., Faioni, E.M., and Mannucci, P.M. (1992) Thrombomodulin is a cofactor for thrombin degradation of recombinant single-chain urokinase plasminogen activator "in vitro" and in a perfused rabbit heart model. *Thromb. Haemost.* **67**, 226–232
5. Bajzar, L., Morser, J., and Nesheim, M. (1996) TAFI, or plasma procarboxypeptidase B, couples the coagulation and fibrinolytic cascades through the thrombin-thrombomodulin complex. *J. Biol. Chem.* **271**, 16603–16608
6. Pekovich, S.R., Bock, P.E., and Hoover, R.L. (2001) Thrombin-thrombomodulin activation of protein C facilitates the activation of progelatinase A. *FEBS Lett.* **494**, 129–132
7. Esmon, N.L., Carroll, R.C., and Esmon, C.T. (1986) Thrombomodulin blocks the ability of thrombin to activate platelets. *J. Biol. Chem.* **258**, 12238–12242
8. Esmon, C.T., Esmon, N.L., and Harris, K.W. (1983) Complex formation between thrombin and thrombomodulin inhibits both thrombin-catalyzed fibrin formation and factor V activation. *J. Biol. Chem.* **257**, 7944–7947
9. Parkinson, J.F., Bang, N.U., and Garcia, J.G. (1993) Recombinant human thrombomodulin attenuates human endothelial cell activation by human thrombin. *Arterioscler. Thromb.* **13**, 1119–1123
10. Li, J., Garnette, C.S., Cahn, M., Claytor, R.B., Rohrer, M.J., Dobson, J.G. Jr., Gerlitz. B., and Cutler, B.S. (2000) Recombinant thrombomodulin inhibits arterial smooth muscle cell proliferation induced by thrombin. *J. Vasc. Surg.* **32**, 804–813
11. Lafay, M., Laguna, R., Le Bonniec, B.F., Lasne, D., Aiach, M., and Rendu, F. (1998) Thrombomodulin modulates the mitogenic response to thrombin of human umbilical vein endothelial cells. *Thromb. Haemost.* **79**, 848–852
12. Nierodzik, M.L., Plotkin, A., Kajumo, F., and Karpatkin, S. (1991) Thrombin stimulates tumor-platelet adhesion *in vitro* and metastasis *in vivo*. *J. Clin. Invest.* **87**, 229–236
13. Nierodzik, M.L., Kajumo, F., and Karpatkin, S. (1992) Effect of thrombin treatment of tumor cells on adhesion of tumor cells to platelets *in vitro* and tumor metastasis *in vivo*. *Cancer Res.* **52**, 3267–3272
14. Esumi, N., Fan, D., and Fidler, J.I. (1991) Inhibition of murine melanoma experimental metastasis by recombinant desulfatohirudin, a highly specific thrombin inhibitor. *Cancer Res.* **51**, 4549–4556
15. Wojtukiewicz, M.Z., Tang, D.G., Ben-Josef, E., Renaud, C., Walz, D.A., and Honn, K.V. (1995) Solid tumor cells express functional 'tethered ligand' thrombin receptor. *Cancer Res.* **55**, 698–704
16. Even-Ram, S., Uziely. B., Cohen, P., Grisaru-Granovsky, S., Maoz, M., Ginzburg, Y., Reich, R., Vlodavsky, I., and Bar-

Shavit, R. (1998) Thrombin receptor overexpression in malignant and physiological invasion processes. *Nat. Med.* **4**, 909–914
17. Hernandez-Rodriguez, N.A., Correa, E., Contreras-Paredes, A., and Green, L. (1999) Evidence that thrombin present in lungs of patients with pulmonary metastasis may contribute to the development of the disease. *Lung Cancer* **26**, 157–167
18. Henrikson, K.P., Salazar, S.L., Fenton, J.W. II., and Pentecost, B.T. (1999) Role of thrombin receptor in breast cancer invasiveness. *Br. J. Cancer* **79**, 401–406
19. Ogawa, H., Yonezawa, S., Maruyama, I., Matsushita, Y., Tezuka, Y., Toyoyama, H., Yanagi, M., Matsumoto, H., Nishijima, H., Shimotakahara, T., Aikou, T., and Sato, E. (2000) Expression of thrombomodulin in squamous cell carcinoma of the lungs: its relationship to lymph node metastasis and prognosis of the patients. *Cancer Lett.* **149**, 95–103
20. Takebayashi, Y., Yamada, K., Maruyama, I., Fujii, R., Akiyama, S., and Aikou, T. (1995) The expression of thymidine phosphorylase and thrombomodulin in human colorectal carcinomas. *Cancer Lett.* **92**, 1–7
21. Ordonez, N.G. (1997) Value of thrombomodulin immunostaining in the diagnosis of transitional cell carcinoma: a comparative study with carcinoembryonic antigen. *Histopathology* **31**, 517–524
22. Ordonez, N.G. (1998) Thrombomodulin expression in transitional cell carcinoma. *Am. J. Clin. Pathol.* **110**, 385–390
23. Matsumoto, M., Natsugoe, S., Nakashima, S., Shimada, M., Nakano, S., Kusano, C., Baba, M., Takao, S., Matsushita, Y., and Aikou, T. (2000) Biological evaluation of undifferentiated carcinoma of the esophagus. *Ann. Surg. Oncol.* **7**, 204–209
24. Suehiro, T., Shimada, M., Matsumata, T., Taketomi, A., Yamamoto, K., and Sugimachi, K. (1995) Thrombomodulin inhibits intrahepatic spread in human hepatocellular carcinoma. *Hepatology* **21**, 1285–1290
25. Wilhelm, S., Schmitt, M., Parkinson, J., Kuhn, W., Graeff, H., and Wilhelm O.G. (1998) Thrombomodulin, a receptor for the serine protease thrombin, is decreased in primary tumors and metastases but increased in ascitic fluids of patients with advanced ovarian cancer FIGO IIIc. *Int. J. Oncol.* **13**, 645–651
26. Lindahl, A.K., Boffa, M.C., and Abildgaard, U. (1993) Increased plasma thrombomodulin in cancer patients. *Thromb. Haemost.* **69**, 112–114
27. Boffa, M.C., Lapeyrere, C., Berard, M., Lindahl, A.K., Flageul, B., Chemaly, P., Abildgaard, U., and Dubertret, L. (1994) Plasma thrombomodulin level in malignancy varies according to the tumor type. *Nouv. Rev. Fr. Hematol.* **36**, S87–88
28. Salmaggi, A., Eoli, M., Frigerio, S., Ciusani, E., Silvani, A., and Boiardi, A. (1999) Circulating intercellular adhesion molecule-1 (ICAM-1), vascular cell adhesion molecule-1 (VCAM-1) and plasma thrombomodulin levels in glioblastoma patients. *Cancer Lett.* **146**, 169–172
29. Liotta, L.A. (1986) Tumor invasion and metastases-role of the extracellular matrix: Rhoads Memorial Award lecture. *Cancer Res.* **46**, 1–7
30. Terranova, V.P., Hujanen, E.S., and Martin, G.R. (1986) Basement membrane and the invasive activity of metastatic tumor cells. *J. Natl Cancer Inst.* **77**, 311–316
31. Gomi, K., Zushi, M., Honda, G., Kawahara, S., Matsuzaki, O., Jr., Kanabayashi, T., Yamamoto, S., Maruyama, I., and Suzuki, K. (1990) Antithrombotic effect of recombinant human thrombomodulin on thrombin-induced thromboembolism in mice. *Blood* **75**, 1396–1399
32. Niimi, S., Oshizawa, T., Naotsuka, M., Ohba, S., Yokozawa, A., Murata, T., and Hayakawa, T. (2002) Establishment of a standard assay method for human thrombomodulin and determination of the activity of the Japanese reference standard. *Biologicals* **30**, 69–76
33. Kawabata, S., Miura, T., Morita, T., Kato, H., Fujikawa, K., Iwanaga, S., Takada, K., Kimura, T., and Sakakibara, S. (1988) Highly sensitive peptide-4-methylcoumaryl-7-amide substrates for blood-clotting proteases and trypsin. *Eur. J. Biochem.* **172**, 17–25
34. Deryugina, E.I., Luo, G.X., Reisfeld, R.A., Bourdon, M.A., and Strongin, A. (1997) Tumor cell invasion through matrigel is regulated by activated matrix metalloproteinase-2. *Anticancer Res.* **17**, 3201–3210
35. Greenwood, F.C., Hunter, W.M., Glover, J.S. (1963) The preparation of ^{131}I-labelled human growth hormone of high specific radioactivity. *Biochem. J.* **89**, 114–123
36. Haeuptle, M.T., Aubert, M.L., Djiane J., Kraehenbuhl, J.P. (1983) Binding sites for lactogenic and somatogenic hormones from rabbit mammary gland and liver. *J. Biol. Chem.* **258**, 305–314
37. Matsushita, Y., Yoshiie, K., Imamura, Y., Ogawa, H., Imamura, H., Takao, S., Yonezawa, S., Aikou, T., Maruyama, I., and Sato, E. (1998) A subcloned human esophageal squamous cell carcinoma cell line with low thrombomodulin expression showed increased invasiveness compared with a high thrombomodulin-expressing clone—thrombomodulin as a possible candidate for an adhesion molecule of squamous cell carcinoma. *Cancer Lett.* **127**, 195–201
38. Hosaka, Y., Higuchi, T., Tsumagari, M., and Ishii, H. (2000) Inhibition of invasion and experimental metastasis of murine melanoma cells by human soluble thrombomodulin. *Cancer Lett.* **161**, 231–240
39. Zhang, Y., Weiler-Guettler, H., Chen, J., Wilhelm, O., Deng, Y., Qiu, F., Nakagawa, K., Klevesath, M., Wilhelm, S., Bohrer, H., Nakagawa, M., Graeff, H., Martin, E., Stern, D.M., Rosenberg, R.D., Ziegler, R., and Nawroth, P.P. (1998) Thrombomodulin modulates growth of tumor cells independent of its anticoagulant activity. *J. Clin. Invest.* **101**, 1301–1309
40. Maruyama, I. and Majerus, P.W. (1985) The turnover of thrombin-thrombomodulin complex in cultured human umbilical vein endothelial cells and A549 lung cancer cells. Endocytosis and degradation of thrombin. *J. Biol. Chem.* **260**, 15432–15438
41. Hart, I.R., Goode, N.T., and Wilson, R.E. (1989) Molecular aspects of the metastatic cascade. *Biochim. Biophys. Acta* **989**, 65–84
42. Wells, A. (2000) Tumor invasion: role of growth factor-induced cell motility. *Adv. Cancer Res.* **78**, 31–101
43. Matrisian, L.M. (1990) Metalloproteinases and their inhibitors in matrix remodeling. *Ternds Genet.* **6**, 121–125
44. Collier, I.E., Wilhelm, S.M., Eisen, A.Z., Marmer, B.L., Grant. G.A., Seltzer. J.L., Kronberger, A., He. C.S., Bauer, E.A., and Goldberg, G.I. (1988) H-ras oncogene-transformed human bronchial epithelial cells (TBE-1) secrete a single metalloprotease capable of degrading basement membrane collagen. *J. Biol. Chem.* **263**, 6579–6587
45. Wilhelm, S.M., Collier, I.E., Marmer, B.L., Eisen, A.Z., Grant, G.A., and Goldberg, G.I. (1989) SV40-transformed human lung fibroblasts secrete a 92-kDa type IV collagenase which is identical to that secreted by normal human macrophages. *J. Biol. Chem.* **264**, 17213–17221
46. Fessler, L.I., Duncan, K.G., Fessler, J.H., Salo, T., and Tryggvason, K. (1984) Identification of the procollagen IV cleavage products produced by a specific tumor collagenase. *J. Biol. Chem.* **259**, 9783–9789
47. Woessner, J.F. Jr. (1991) Matrix metalloproteinases and their inhibitors in connective tissue remodeling. *FASEB J.* **5**, 2145–2154
48. Senior, R.M., Griffin, G.L., Fliszar, C.J., Shapiro, S.D., Goldberg, G.I., and Welgus, H.G. (1991) Human 92- and 72-kilodalton type IV collagenases are elastases. *J. Biol. Chem.* **266**, 7870–7875
49. Murphy, G., Cockett, M.I., Ward, R.V., and Docherty, A.J. (1991) Matrix metalloproteinase degradation of elastin, type IV collagen and proteoglycan. A quantitive comparison of the activities of 95 kDa and 72 kDa gelatinases, stromelysins-1 and -2 and punctuated metalloproteinae (PUMP). *Biochem. J.* **277**, 277–279
50. Nguyen, Q., Murphy, G., Hughes, C.E., Mort, J.S., and Roughley, P.J. (1993) Matrix metalloproteinases cleave at two distinct sites on human cartilage link protein. *Biochem. J.* **295**, 595–598

51. Fosang, A.J., Last, K., Knauper, V., Neame, P.J., Murphy, G., Hardingham, T.E., Tschesche, H., and Hamilton, J.A. (1993) Fibroblast and neutrophil collagenases cleave at two sites in the cartilage aggrecan interglobular domain. *Biochem. J.* **295**, 273–276
52. Sires, U.I., Griffin, G.L., Broekelmann, T.J., Mecham, R.P., Murphy, G., Chung, A.E., Welgus, H.G., and Senior, R.M. (1993) Degradation of entactin by matrix metalloproteinases. Susceptibility to matrilysin and identification of cleavage sites. *J. Biol. Chem.* **268**, 2069–2074
53. Zucker, S., Conner, C., DiMassmo, B.I., Ende, H., Drews, M., Seiki, M., and Bahou, W.F. (1995) Thrombin induces the activation of progelatinase A in vascular endothelial cells. Physiologic regulation of angiogenesis. *J. Biol. Chem.* **270**, 23730–23738
54. Galis, Z.S., Kranzhofer, R., Fenton, J.W. II., and Libby, P. (1997) Thrombin promotes activation of matrix metalloproteinase-2 produced by cultured vascular smooth muscle cells. *Arterioscler. Thromb. Vasc. Biol.* **17**, 483–489
55. Nguyen, M., Arkell, J., and Jackson, C.J. (1999) Thrombin rapidly and efficiently activates gelatinase A in human microvascular endothelial cells via a mechanism independent of active MT1 matrix metalloproteinase. *Lab. Invest.* **79**, 467–475
56. Pekovich, S.R., Bock, P.E., and Hoover, R.L. (2001) Thrombin-thrombomodulin activation of protein C facilitates the activation of progelatinase A. *FEBS Lett.* **694**, 129–132
57. Lafleur, M.A., Hollenberg, M.D., Atkinson. S.J., Knauper, V., Murphy, G., and Edwards, D.R. (2001) Activation of pro-(matrix metalloproteinase-2) (pro-MMP-2) by thrombin is membrane-type-MMP-dependent in human umbilical vein endothelial cells and generates a distinct 63 kDa active species. *Biochem. J.* **357**, 107–115
58. Maragoudakis, M.E., Kraniti, N., Giannopoulou, E., Alexopoulos, K., and Matsuokas, J. (2001) Modulation of angiogenesis and progelatinase A by thrombin receptor mimetics and antagonists. *Endothelium* **8**, 195–205
59. Liu, Y., Gilcrease, M.Z., Henderson, Y., Yuan, X.H., Clayman, G.L., and Chen, Z. (2001) Expression of protease-activated receptor 1 in oral squamous cell carcinoma. *Cancer Lett.* **169**, 173–180
60. Stetler-Stevenson, W.G., Aznavoorian, S., and Liotta, L.A. (1993) Tumor cell interactions with the extracellular matrix during invasion and metastasis. *Annu. Rev. Cell. Biol.* **9**, 541–573
61. Himelstein, B.P., Canete-Soler, R., Bernhard, E.J., Dilks, D.W., and Muschel, R.J. (1994) Metalloproteinases in tumor progression: the contribution of MMP-9. *Invasion Metastasis.* **14**, 246–258
62. Bernhard, E.J., Gruber, S.B., and Muschel, R.J. (1994) Direct evidence linking expression of matrix metalloproteinase 9 (92-kDa gelatinase/collagenase) to the metastatic phenotype in transformed rat embryo cells. *Proc. Natl Acad. Sci. USA* **91**, 4293–4297
63. MacDougall, J.R., and Matrisian. L.M. (1995) Contribution of tumor and stromal matrix metalloroteinases to tumor progression, invasion and metastasis. *Cancer Metastasis Rev.* **14**, 351–362
64. Hua, J. and Muschel, R.J. (1996) Inhibition of matrix metalloproteinase 9 expression by a ribozyme blocks metastasis in a rat sarcoma model system. *Cancer Res.* **56**, 5279–5284
65. Kim, J., Yu, W., Kovalski, K., and Ossowski, L. (1998) Requirement for specific proteases in cancer cell intravasation as revealed by a novel semiquantitative PCR-based assay. *Cell* **94**, 353–362
66. Hahn-Dantona, E., Ramos-DeSimone, N., Sipley, J., Nagase, H., French, D.L., and Quigley, J.P. (1999) Activation of proMMP-9 by a plasmin/MMP-3 cascade in a tumor cell model. Regulation by tissue inhibitors of metalloproteinases. *Ann. N. Y. Acad. Sci.* **878**, 372–387
67. John, A. and Tuszynski, G. (2001) The role of matrix metalloproteinases in tumor angiogenesis and tumor metastasis. *Pathol. Oncol. Res.* **7**, 14–23
68. Giannelli, G. and Antonaci, S. (2002) Gelatinases and their inhibitors in tumor metastasis: from biological research to medical applications. *Histol. Histopathol.* **17**, 339–345
69. Fernandez-Patron, C., Zhang, Y., Radomski, M.W., Hollenberg, M.D., and Davidge, S.T. (1999) Rapid release of matrix metalloproteinase (MMP)-2 by thrombin in the rat aorta: modulation by protein tyrosine kinase/phosphatase. *Thromb. Haemost.* **82**, 1353–1357
70. Duhamel-Clérin, E., Orvain, C., Lanza, F., Cazenave, J.P., and Klein-Soyer, C. (1997) Thrombin receptor-mediated increase of two matrix metalloproteinases, MMP-1 and MMP-3, in human endothelial cells. *Arterioscler. Thromb. Vasc. Biol.* **17**, 1931–1938
71. Liu, W.H., Chen, X.M., and Fu, B. (2000) Thrombin stimulates MMP-9 mRNA expression through AP-1 pathway in human mesangial cells. *Acta. Pharmacol. Sin.* **21**, 641–645
72. Yoshida, E., Verrusio, E.N., Mihara, H., Oh, D., and Kwaan, H.C. (1994) Enhancement of the expression of urokinase-type plasminogen activator from PC-3 human prostate cancer cells by thrombin. *Cancer Res.* **54**, 3300–3304
73. Benezra, M., Vlodavsky, I., and Bar-Shavit, R. (1992) Thrombin enhances degradation of heparan sulfate in the extracellular matrix by tumor cell heparanase. *Exp. Cell Res.* **201**, 208–215

Expression of Annexin A3 in Primary Cultured Parenchymal Rat Hepatocytes and Inhibition of DNA Synthesis by Suppression of Annexin A3 Expression Using RNA Interference

Shingo NIIMI,*[a] Mizuho HARASHIMA,[b] Masaru GAMOU,[b] Masashi HYUGA,[a] Taiichiro SEKI,[b] Toyohiko ARIGA,[b] Toru KAWANISHI,[a] and Takao HAYAKAWA[c]

[a] *Division of Biological Chemistry and Biologicals, National Institute of Health Sciences; 1–18–1 Kamiyoga, Setagaya-ku, Tokyo 158–8501, Japan:* [b] *Department of Nutrition and Physiology, Nihon University College of Bioresource Sciences; Kameino, Fujisawa 252–8510, Japan; and* [c] *Deputy Director General, National Institute of Health Sciences; 1–18–1 Kamiyoga, Setagaya-ku, Tokyo 158–8501, Japan.*

Received October 30, 2004; accepted January 5, 2005; published online January 7, 2005

Annexin A3 is a member of the lipocortin/annexin family, which binds to phospholipids and membranes in a Ca^{2+}-dependent manner. Although annexin A3 has various functions *in vitro*, its cellular significance is completely unknown. Annexin A3 is not found in rat liver *in vivo*. In the present study, we investigated the expression of annexin A3 in primary cultured parenchymal rat hepatocytes. Annexin A3 protein was detected in 48-h, but not 2.5-h, cultured hepatocytes using Western blot analysis. The annexin A3 level further increased after an additional 24 h of culture. Annexin A3 mRNA was not detected in 2.5-h cultured hepatocytes but was detected 22 h after the start of culture by RT-PCR analysis, reaching a maximum value after 48 h of culture. To define the role of Annexin A3 in DNA synthesis, RNA interference was used to reduce annexin III gene expression in hepatocytes. The transfection of small interfering RNAs targeting annexin A3 in the hepatocytes reduced the corresponding mRNA and protein expression by approximately 80% and more than 90%, respectively, at 24 h after transfection. In the annexin A3 small interfering RNAs-transfected cells, DNA synthesis, as assessed by [^{3}H]thymidine incorporation, decreased by approximately 70% not only in the control cultures, but also in the hepatocyte growth factor- or epidermal growth factor-treated cells. These findings show that annexin A3 is expressed in primary cultured parenchymal rat hepatocytes and that the suppression of annexin A3 expression using RNA interference inhibits DNA synthesis.

Key words annexin A3; RNAi; DNA synthesis; primary cultured hepatocyte; hepatocyte growth factor (HGF); epidermal growth factor (EGF)

Annexin (Anx) A3 is also called "lipocortin 3" or "placental anticoagulant protein 3" (PAP-III)[1] and is a member of the lipocortin/annexin family, which binds to phospholipids and membranes in a Ca^{2+}-dependent manner.[2—4] AnxA3 has been shown to have anticoagulant and anti-phospholipase A_2 properties *in vitro*[5] and to promote the Ca^{2+}-dependent aggregation of isolated specific granules from human neutrophils.[6] Although the physiological functions of other annexins have been recently clarified in knock-out and transgenic models,[7—14] the functions of AnxA3 are completely unknown.[15]

Recently, we found that AnxA3 protein and its mRNA are not expressed in isolated parenchymal rat hepatocytes.[16,17] Consistent with these findings, AnxA3 protein and its mRNA are not detectable by Western blot analysis and Northern blot analysis in rat liver.[18—21] However, there have been no reports on the behavior of AnxA3 in primary cultured parenchymal rat hepatocytes. In the present study, we investigated the expression and function of AnxA3 in cultured parenchymal rat hepatocytes.

MATERIALS AND METHODS

Materials Recombinant human hepatocyte growth factor (HGF) was purchased from R&D systems (Minneapolis, MN, U.S.A.). Mouse epidermal growth factor (EGF) was purchased from Wako (Osaka, Japan). [^{3}H]thymidine (79.9 Ci/mmol) was purchased from PerkinElmer (Boston, MA, U.S.A.). Rabbit anti-human ANXA3 antibody serum was a generous gift from Dr. F. Russo-Marie and Dr. C. Raguenness-Nicol.

Cell Isolation and Monolayer Cultures Parenchymal hepatocytes were isolated from adult male Wistar rats, weighing 180—200 g, by *in situ* perfusion of the liver with collagenase.[22] All animal care and procedure protocols were approved by the institutional care committee. The cells were then suspended at a density of 2.5×10^5 cells/ml in Williams E medium (WE) containing 5% fetal bovine serum and 1 nM insulin and cultured at a density of 0.5×10^5 cells/cm^2 in a 6 cm dish and a 48-well microplate precoated with collagen type-I AC in a humidified chamber at 37 °C in 5% CO_2 and 30% O_2 in air. Cells plated in the 6-cm dish and 48-well microplate were used to prepare total cellular extracts or total RNA and to measure DNA synthesis, respectively. After 2.5 h of culture, the medium was replaced with a serum- and hormone-free medium containing aprotinin (1 μg/ml).

Western Blot Analysis Cell lysates were prepared using a modification of a previously described method.[23] The cells were washed with phosphate-buffered saline (PBS) followed by buffer A (50 mM Tris–HCl [pH 7.5], 150 mM NaCl, and 10 mM EDTA). The cells were then harvested after the addition of 20 μl of buffer A. The cells were suspended, shaken for 15 min at room temperature, and sonicated five times for 15 s each time while in an ice bath after the addition of 1/5 [v/v] of 5×buffer A containing 2.5% Triton X-100 and 1/100 [v/v] of a protease inhibitor cocktail (SIGMA). After centrifugation at 100000×g, the cytosolic fraction (about 25 μg) was subjected to sodium dodecyl sulfate-polyacrylamide gel

* To whom correspondence should be addressed. e-mail: niimi@nihs.go.jp

electrophoresis on a 10% gel and electroblotted to a PVDF membrane (GVHP; Millipore). After blocking the membrane with 5% skimmed milk, a Western blot analysis was performed using rabbit anti-human AnxA3 antibody serum at a dilution of 1 : 18000; detection was performed using the ECL detection system (Amersham Bioscience).

Reverse Transcription Polymerase Chain Reaction Analysis Total RNA was exctracted from the cells using Trizol reagent (Invitrogen) according to the manufacturer's protocols. Approximately 3 μg of RNA per sample was reverse-transcribed using the THERMOSCRIPT™ RT-PCR System (Invitrogen) and oligo$(dT)_{20}$ in a final volume of 40 μl, according to the manufacturer's protocols. Subsequently, 1 μl of cDNA was polymerase chain reaction (PCR)-amplified using the THERMOSCRIPT™ RT-PCR System (Invitrogen) in a final volume of 20 μl per reaction, according to the manufacturer's protocols, for 14—23 cycles of denaturation for 30 s at 94 °C, annealing for 30 s at 60 °C, and polymerization for 1 min at 72 °C using Anx AIII or glyceraldehyde 3-phosphate dehydrogenase (GAPDH) cDNA specific primers under linear conditions. The PCR products were separated on a 2% agarose gel, stained with SYBR Green I, and visualized and analyzed with a FluorolImager 595 (Amersham Bioscience). A computer assisted-analyzer was used to quantitatively analyze the signals, and the signals were normalized to the signal of a house keeping gene, the gene coding GAPDH. The sequences of the AnxA3 primers were as follows: 5′-CAAATTCACCGAGATCCTGT-3′ and 5′-TGCTGGAGTGCTGTACGAAA-3′. The sequences of the GAPDH primers were as follows: 5′-ACCACAGTCCATGCCATCAC-3′ and 5′-TCCACCACCTGTTGCTGTA-3′.[24] The PCR product specificity was confirmed by DNA sequence analysis using an ABI Prism 377 DNA Sequencer (Applied Biosystems, Foster City, CA, U.S.A.).

Preparation and Transfection of Small Interfering RNAs Targeting AnxA3 Small interfering RNAs (siRNAs) targeting rat AnxA3 were designed according to the guidelines of the "Dharmacon siDESIGN Center" (www.dharmacon.com) and obtained from Dharmacon Research (Lafayette) in annealed and lyophilized forms. The target sequences were localized at positions, 493 and 690 bps downstream of the start codon. The sequences of each siRNA pair were as follows: AnxA3 siRNA 1, 5′-GAG ACG AAA GCC UGA AAG UdTdT-3′ and ACU UUC AGG CUU UCG UCU cdTdT-3′; ANXA3 siRNA 2, 5′-GGA GAA UUA UCU GGG CAU UdTdT-3′ and AAU GCC CAG AUA AUUCUC cdTdT-3; and control siRNA, 5′-ACU CUA UCU GCA CGC UGA CUU-3′ and 5′-P G UCA GCG UGC AGA UAG AGU UU-3′. No homology between any relevant mammalian gene and the control siRNA was observed. These siRNAs were dissolved in an RNase-free solution provided by Dharmacon Research at a concentration of 20 μM. After 20 h of cell culture, the medium was replaced with WE containing aprotinin (1 μg/ml) immediately prior to transfection. Transfection with siRNA was performed using SiFector (B-bridge), according to the user guidelines. Sixty microliters of both AnxA3 siRNA 1 and 2 were diluted with OPTI-MEM (Invitrogen) to a final volume of 400 μl. Sixty-four microliters of SiFector was also diluted in OPTI-MEM to a final volume of 400 μl, then suspended and incubated at room temperature for 5 min. Next, the diluted siRNA was combined with SiFector, and the mixture was incubated at room temperature to allow the siRNA-SiFector complex to form. Eight hundred microliters of the siRNA-SiFector complex was added to the cultures (6-cm dish). For the 48-well plates, the siRNA-SiFector complex was prepared as described above except that the volume of each solution per well was scaled down to 1/16.

Measurement of [^{3}H]thymidine Incorporation After 20 h of culture, the medium was replaced with hormone-free medium containing aprotinin (1 μg/ml) and 0.1% bovine serum albumin (BSA), and EGF (2 ng/ml) or HGF (20 ng/ml) was added. After 1 h, 50 μl of siRNA-SiFector complex, prepared as described above, was added to the wells. After another 24 h, [^{3}H]thymidine (0.626 μCi) and thymidine (676.6 ng) were added, and 10 μg/ml of aphidicolin was added to some wells at the same time. The cells were then cultured for another 24 h. [^{3}H]thymidine incorporation was measured as described previously.[25] The difference between the radioactivity in the hot-trichloroacetic acid soluble fraction with and without aphidicolin was calculated as dpm/mg protein. Cell protein was measured using a previously described method,[26] with BSA used as a standard.

RESULTS

Expression of AnxA3 during Culture At first, we investigated the expression of AnxA3 in primary cultured parenchymal rat hepatocytes. AnxA3 protein was not detected by Western blot analysis 2.5 and 24 h after the start of culture but was detected after 48 h of culture (Fig. 1A). The level after 72 h of culture was approximately 1.6-fold higher than that after 48 h of culture (Fig. 1B). AnxA3 mRNA was not detected by reverse transcription (RT)-PCR in cultured hepatocytes after 2.5 h of culture but was significantly detected after 22 h of culture (Fig. 2A), reaching a maximum value after 48 h of culture (Fig. 2B). These results indicate

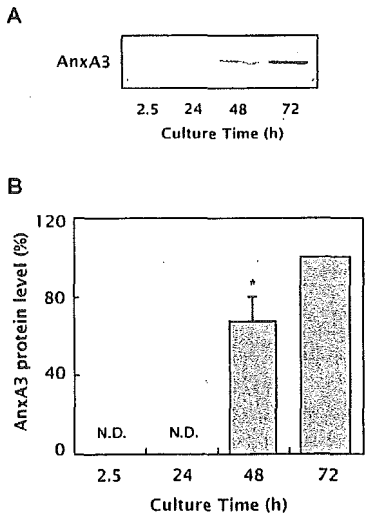

Fig. 1. Expression of AnxA3 Protein during Culture

(A) The data shown are representative of the Western blot analysis results. Cells lysates were prepared from the cells at the indicated times and used for the Western blot analysis. (B) The intensity of each band was quantified, and the results are shown relative to the value of cells cultured for 72 h. The data are expressed as the mean±S.D. of 3 experiments. *$p<0.01$, compared with the value of cells cultured for 72 h. N.D., not detected.

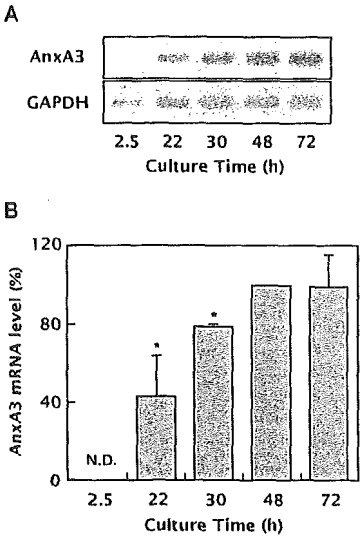

Fig. 2. Increase in AnxA3 mRNA Level during Culture

(A) The data shown are representative of the RT-PCR analysis results. Total RNA was prepared from the cells at the indicated times and used for the RT-PCR analysis. (B) The intensity of each band was quantified, and the results are shown relative to the value of cells cultured for 48 h. The data are expressed as the mean±S.D. of 3 experiments. *$p<0.01$, compared with the value of cells cultured for 48 h. N.D., not detected.

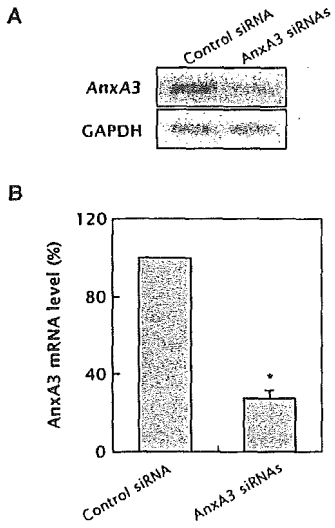

Fig. 3. Suppression of Increase in AnxA3 mRNA Level during Culture with RNAi

(A) The data shown are representative of the RT-PCR analysis results. Total RNA was prepared from the cells 1 d after siRNA transfection and used for the RT-PCR analysis. (B) The intensity of each band was quantified, and the results are shown relative to the value of cells transfected with control siRNA. The data are expressed as the mean±S.D. of 3 experiments. *$p<0.01$, compared with the value of cells transfected with control siRNA.

that the expression of AnxA3 is regulated by its mRNA level.

Suppression of AnxA3 Expression Using RNA Interference Next, we attempted to suppress AnxA3 expression by RNA interference (RNAi) to examine the role of ANXA3 in the cultured hepatocytes. AnxA3 mRNA expression was markedly reduced by treatment with AnxA3 siRNAs, compared with the expression after treatment with control siRNA, 1 d after the transfection (Fig. 3A), with an inhibition of approximately 80% (Fig. 3B). Furthermore, the AnxA3

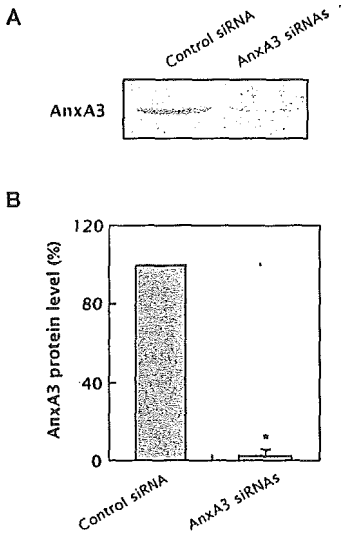

Fig. 4. Suppression of AnxA3 Protein Expression during Culture with RNAi

(A) The data shown are representative of the Western blot analysis results. Cells lysates were prepared from the cells 1 d after siRNA transfection and used for the Western blot analysis. (B) The intensity of each band was quantified, and the results are shown relative to the value of cells transfected with control siRNA. The data are expressed as the mean±S.D. of 3 experiments. *$p<0.01$, compared with the value of cells transfected with control siRNA.

protein level was also reduced by the treatment with AnxA3 siRNAs compared with the level after treatment with control siRNA (Fig. 4A), with an inhibition of more than 95% (Fig. 4B). On the other hand, the control siRNA had almost no effect on AnxA3 protein and mRNA levels compared with those treated with SiFector alone (data not shown). Neither the control nor AnxA3 siRNAs caused any cytotoxic effects, as observed microscopically or by the quantification of the total amount of protein in each sample (data not shown). These results indicate that AnxA3 siRNAs efficiently and specifically, inhibit the expression of AnxA3 in primary cultured parenchymal rat hepatocytes.

Inhibition of DNA Synthesis by Suppression of AnxA3 Expression Using RNAi Finally, we examined the role of AnxA3 in DNA synthesis by suppressing AnxA3 expression using RNAi. EGF (2 ng/ml) and HGF (20 ng/ml) stimulated DNA synthesis by approximately 7-fold and 9-fold, respectively in hepatocytes treated with control siRNA (Fig. 5). The stimulations were inhibited to approximately 70% by treatment with AnxA3 siRNAs. Similar results were also obtained in the control cells, whereas the control siRNA had almost no effect on DNA synthesis, compared with the effect in cells treated with SiFector alone (data not shown).

DISCUSSION

In the present study, we showed for the first time that AnxA3 is expressed in cultured parenchymal rat hepatocytes and that the inhibition of AnxA3 expression by RNAi resulted in a significant inhibition of DNA synthesis, suggesting that the expression of AnxA3 is necessary for DNA synthesis in primary cultured parenchymal rat hepatocytes.

Hepatocytes placed under culture conditions, are known to acquire a growth potential characterized by the enhancement of DNA synthesis, which is caused by several growth

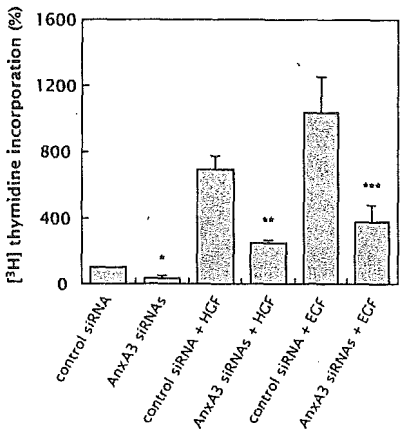

Fig. 5. Inhibition of DNA Synthesis by RNAi

The results are shown relative to the value of control cultured cells transfected with control siRNA. The data are expressed as the mean±S.D. of duplicate wells in 3 experiments. *$p<0.01$, compared with the value of control cultured cells transfected with control siRNA. **$p<0.01$, compared with the value of cells cultured in the presence of HGF and transfected with control siRNA. ***$p<0.01$, compared with the value of cells cultured in the presence of EGF and transfected with control siRNA. The mean±S.D. of [^{3}H]thymidine incorporation in the control cultured cells transfected with control siRNA was $9.72\times10^4\pm0.68\times10^4$ dpm/mg protein.

factors.[27,28] Our present findings suggest that the expression of AnxA3 is partly necessary for hepatocytes to acquire a growth potential under culture conditions. In fact, the enhanced expression of AnxA3 has been observed in hepatocellular carcinoma cell lines.[29] In addition, we discovered that the enhanced expression of Anx3 was observed in the proliferative hepatocytes after carbon tetrachloride-induced rat liver damage (unpublished observations).

As for other annexins, several findings concerning the relation of AnxA1 to hepatocyte growth has been reported as described below. The suppression of AnxA1 expression using antisense technology inhibited proliferation in a mouse hepatocyte cell line.[30] AnxA1 increased in the proliferative hepatocytes after carbon tetrachloride-induced rat liver damage or a partial hepatectomy and in hepatocellullar carcinoma tissue.[31,32]

Although the mechanism of action of AnxA3 on DNA synthesis is presently uncertain, the target of AnxA3 may be a common signal transduction pathway, and not necessarily a constitutive or growth factor-mediated one, because the suppression of AnxA3 expression using RNAi not only inhibited the control of DNA synthesis, but also EGF- or HGF-stimulated DNA synthesis, almost to a similar level. In this respect, the findings described below may be relevant to speculations on the mechanism of action of AnxA3 on DNA synthesis. The growth factor-mediated enhancement of hepatocyte growth consists of several signal transduction pathways.[33] The activation of cytosolic phospholipase A_2 ($cPLA_2$) by MAP kinase liberates arachidonic acid from phospholipids and is followed by the generation of prostaglandins, mediators of DNA synthesis, *via* cyclooxygenase. Interestingly, the suppression of AnxA1 expression using antisense technology inhibited $cPLA_2$ activity in a mouse hepatocyte cell line.[30] This report suggests that $cPLA_2$ must be phosphorylated by AnxA1 to become active. Additional evidence suggests that AnxA1 (275—346 aa), the region responsible for phospholipid binding is necessary for the interaction between AnxA1 and $cPLA_2$.[34] Further study is required to clarify the mechanism of action of AnxA3, including the possibility that AnxA3 positively modulates $cPLA_2$ activity, as in the case of AnxA1.

Acknowledgements This work was supported by grants for Health and Welfare Research from the Japanese Ministry of Health, Labor and Welfare.

REFERENCES

1) Crumpton M. J., Dedman J. R., *Nature* (London), **345**, 212 (1990).
2) Raynal P., Pollard H. B., *Biochim. Biophys. Acta*, **1197**, 63—93 (1994).
3) Gerke V., Moss S. E., *Physiol. Rev.*, **82**, 331—371 (2002).
4) Moss S. E., Morgan R. O., *Genome Biol.*, **5**, 219. 1—8 (2004).
5) Tait J. F., Sakata M., McMullen B. A., Miao C. H., Funakoshi T., Hendrickson L. E., Fujikawa K., *Biochemistry*, **27**, 6268—6276 (1988).
6) Ernst J. D., Hoye E., Blackwood R. A., Jaye D., *J. Clin. Invest.*, **85**, 1065—1071 (1990).
7) Gunteski-Hamblin A. M., Song G., Walsh R. A., Frenzke M., Boivin G. P., Dorn G. W., 2nd, Kaetzel M. A., Horseman N. D., Dedman J. R., *Am. J. Physiol.*, **270**, H1091—1100 (1996).
8) Kubista H., Hawkins T. E., Patel D. R., Haigler H. T., Moss S. E., *Curr. Biol.*, **9**, 1403—1406 (1999).
9) Srivastava M., Atwater I., Glasman M., Leighton X., Goping G., Caohuy H., Miller G., Pichel J., Westphal H., Mears D., Rojas E., Pollard H. B., *Proc. Natl. Acad. Sci. U.S.A.*, **96**, 13783—13788 (1999).
10) Herr C., Smyth N., Ullrich S., Yun F., Sasse P., Hescheler J., Fleischmann B., Lasek K., Brixius K., Schwinger R. H., Fassler R., Schroder R., Noegel A. A., *Mol. Cell. Biol.*, **21**, 4119—4128 (2001).
11) Song G., Harding S. E., Duchen M. R., Tunwell R., O'Gara P., Hawkins T. E., Moss S. E., *Faseb. J.*, **16**, 622—624 (2002).
12) Roviezzo F., Getting S. J., Paul-Clark M. J., Yona S., Gavins F. N., Perretti M., Hannon R., Croxtall J. D., Buckingham J. C., Flower R. J., *J. Physiol. Pharmacol.*, **53**, 541—553 (2002).
13) Hannon R., Croxtall J. D., Getting S. J., Roviezzo F., Yona S., Paul-Clark M. J., Gavins F. N., Perretti M., Morris J. F., Buckingham J. C., Flower R. J., *Faseb. J.*, **17**, 253—255 (2003).
14) Croxtall J. D., Gilroy D. W., Solito E., Choudhury Q., Ward B. J., Buckingham J. C., Flower R. J., *Biochem. J.*, **371**, 927—935 (2003).
15) Rand J. H., *N. Engl. J. Med.*, **340**, 1035—1036 (1999).
16) Niimi S., Hyuga M., Harashima M., Seki T., Ariga T., Kawanishi T., Hayakawa T., *Biol. Pharm. Bull.*, **27**, 1864—1868 (2004).
17) Niimi S., Oshizawa T., Yamaguchi T., Harashima M., Seki T., Ariga T., Kawanishi T., Hayakawa T., *Biochem. Biophys. Res. Commun.*, **300**, 770—774 (2003).
18) Kaetzel M. A., Hazarika P., Dedman J. R., *J. Biol. Chem.*, **264**, 14463—14470 (1989).
19) Comera C., Rothhut B., Cavadore J. C., Vilgrain I., Cochet C., Chambaz E., Russo-Marie F., *J. Cell. Biochem.*, **40**, 361—370 (1989).
20) Kristensen B. I., Kristensen P., Johnsen A. H., *Int. J. Biochem.*, **25**, 1195—1202 (1993).
21) Pepinsky R. B., Tizard R., Mattaliano R. J., Sinclair L. K., Miller G. T., Browning J. L., Chow E. P., Burne C., Huang K. S., Pratt D., Wachter L., Hession C., Frey A. Z., Wallner B. P., *J. Biol. Chem.*, **263**, 10799—10811 (1988).
22) Tanaka K., Sato M., Tomita Y., Ichihara A., *J. Biochem.* (Tokyo), **84**, 937—946 (1978).
23) Romisch J., Schuler E., Bastian B., Burger T., Dunkel F. G., Schwinn A., Hartmann A. A., Paques E. P., *Blood Coagul. Fibrinolysis*, **3**, 11—17 (1992).
24) Uno S., Nakamura M., Seki T., Ariga T., *Biochem. Biophys. Res. Commun.*, **239**, 123—128 (1997).
25) Niimi S., Horikawa M., Seki T., Ariga T., Kobayashi T., Hayakawa T., *Biol. Pharm. Bull.*, **25**, 437—440 (2002).
26) Bradford M. M., *Anal. Biochem.*, **72**, 248—254 (1976).
27) Fausto N., Laird A. D., Webber E. M., *Faseb. J.*, **9**, 1527—1536 (1995).
28) Michalopoulos G. K., DeFrances M. C., *Science*, **276**, 60—66 (1997).
29) Liang R. C., Neo J. C., Lo S. L., Tan G. S., Seow T. K., Chung M. C., *J. Chromatogr. B Analyt. Technol. Biomed. Life Sci.*, **771**, 303—328 (2002).
30) de Coupade C., Gillet R., Bennoun M., Briand P., Russo-Marie F.,

Solito E., *Hepatology*, **31**, 371—380 (2000).
31) Masaki T., Tokuda M., Fujimura T., Ohnishi M., Tai Y., Miyamoto K., Itano T., Matsui H., Watanabe S., Sogawa K., Yamada T., Konishi R., Nishioka M., Hatase O., *Hepatology*, **20**, 425—435 (1994).
32) Masaki T., Tokuda M., Ohnishi M., Watanabe S., Fujimura T., Miyamoto K., Itano T., Matsui H., Arima K., Shirai M., Maeba T., Sogawa K., Konishi R., Taniguchi K., Hatanaka Y., Hatase O., Nishioka M., *Hepatology*, **24**, 72—81 (1996).
33) Adachi T., Nakashima S., Saji S., Nakamura T., Nozawa Y., *Hepatology*, **21**, 1668—1674 (1995).
34) Kim S. W., Rhee H. J., Ko J., Kim Y. J., Kim H. G., Yang J. M., Choi E. C., Na D. S., *J. Biol. Chem.*, **276**, 15712—15719 (2001).